University Transportation Research Center - Region 2

Final Report

Finite Element Simulation of Truck Impacts on Highway Bridge Piers

Performing Organization: The City College of New York

April 2016

Sponsor:
Research and Innovative Technology Administration/USDOT

University Transportation Research Center - Region 2

The Region 2 University Transportation Research Center (UTRC) is one of ten original University Transportation Centers established in 1987 by the U.S. Congress. These Centers were established with the recognition that transportation plays a key role in the nation's economy and the quality of life of its citizens. University faculty members provide a critical link in resolving our national and regional transportation problems while training the professionals who address our transportation systems and their customers on a daily basis.

The UTRC was established in order to support research, education and the transfer of technology in the field of transportation. The theme of the Center is "Planning and Managing Regional Transportation Systems in a Changing World." Presently, under the direction of Dr. Camille Kamga, the UTRC represents USDOT Region II, including New York, New Jersey, Puerto Rico and the U.S. Virgin Islands. Functioning as a consortium of twelve major Universities throughout the region, UTRC is located at the CUNY Institute for Transportation Systems at The City College of New York, the lead institution of the consortium. The Center, through its consortium, an Agency-Industry Council and its Director and Staff, supports research, education, and technology transfer under its theme. UTRC's three main goals are:

Research

The research program objectives are (1) to develop a theme based transportation research program that is responsive to the needs of regional transportation organizations and stakeholders, and (2) to conduct that program in cooperation with the partners. The program includes both studies that are identified with research partners of projects targeted to the theme, and targeted, short-term projects. The program develops competitive proposals, which are evaluated to insure the mostresponsive UTRC team conducts the work. The research program is responsive to the UTRC theme: "Planning and Managing Regional Transportation Systems in a Changing World." The complex transportation system of transit and infrastructure, and the rapidly changing environment impacts the nation's largest city and metropolitan area. The New York/New Jersey Metropolitan has over 19 million people, 600,000 businesses and 9 million workers. The Region's intermodal and multimodal systems must serve all customers and stakeholders within the region and globally.Under the current grant, the new research projects and the ongoing research projects concentrate the program efforts on the categories of Transportation Systems Performance and Information Infrastructure to provide needed services to the New Jersey Department of Transportation, New York City Department of Transportation, New York Metropolitan Transportation Council , New York State Department of Transportation, and the New York State Energy and Research Development Authorityand others, all while enhancing the center's theme.

Education and Workforce Development

The modern professional must combine the technical skills of engineering and planning with knowledge of economics, environmental science, management, finance, and law as well as negotiation skills, psychology and sociology. And, she/he must be computer literate, wired to the web, and knowledgeable about advances in information technology. UTRC's education and training efforts provide a multidisciplinary program of course work and experiential learning to train students and provide advanced training or retraining of practitioners to plan and manage regional transportation systems. UTRC must meet the need to educate the undergraduate and graduate student with a foundation of transportation fundamentals that allows for solving complex problems in a world much more dynamic than even a decade ago. Simultaneously, the demand for continuing education is growing – either because of professional license requirements or because the workplace demands it – and provides the opportunity to combine State of Practice education with tailored ways of delivering content.

Technology Transfer

UTRC's Technology Transfer Program goes beyond what might be considered "traditional" technology transfer activities. Its main objectives are (1) to increase the awareness and level of information concerning transportation issues facing Region 2; (2) to improve the knowledge base and approach to problem solving of the region's transportation workforce, from those operating the systems to those at the most senior level of managing the system; and by doing so, to improve the overall professional capability of the transportation workforce; (3) to stimulate discussion and debate concerning the integration of new technologies into our culture, our work and our transportation systems; (4) to provide the more traditional but extremely important job of disseminating research and project reports, studies, analysis and use of tools to the education, research and practicing community both nationally and internationally; and (5) to provide unbiased information and testimony to decision-makers concerning regional transportation issues consistent with the UTRC theme.

Project No(s):
UTRC/RF Grant No: 49111-09-22

Project Date: April 2016

Project Title: Finite Element Simulation of Truck Impacts on Highway Bridge Piers

Project's Website:
http://www.utrc2.org/research/projects/finite-element-simulation-of-truck

Principal Investigator(s):
Dr. Anil Agrawal
Associate Professor of Civil Engineering
The City College of New York
New York, NY 10031
Tel: (212) 650-8442
Email: anil@ce.ccny.cuny.edu

Co-author(s):
Xiaochen Xu

Performing Organization:
The City College of New York

Sponsor(s):
Research and Innovative Technology Administration/USDOT

To request a hard copy of our final reports, please send us an email at utrc@utrc2.org

Mailing Address:

University Transportation Reserch Center
The City College of New York
Marshak Hall, Suite 910
160 Convent Avenue
New York, NY 10031
Tel: 212-650-8051
Fax: 212-650-8374
Web: www.utrc2.org

Board of Directors

The UTRC Board of Directors consists of one or two members from each Consortium school (each school receives two votes regardless of the number of representatives on the board). The Center Director is an ex-officio member of the Board and The Center management team serves as staff to the Board.

City University of New York
Dr. Hongmian Gong - Geography/Hunter College
Dr. Neville A. Parker - Civil Engineering/CCNY

Clarkson University
Dr. Kerop D. Janoyan - Civil Engineering

Columbia University
Dr. Raimondo Betti - Civil Engineering
Dr. Elliott Sclar - Urban and Regional Planning

Cornell University
Dr. Huaizhu (Oliver) Gao - Civil Engineering

Hofstra University
Dr. Jean-Paul Rodrigue - Global Studies and Geography

Manhattan College
Dr. Anirban De - Civil & Environmental Engineering
Dr. Matthew Volovski - Civil & Environmental Engineering

New Jersey Institute of Technology
Dr. Steven I-Jy Chien - Civil Engineering
Dr. Joyoung Lee - Civil & Environmental Engineering

New York University
Dr. Mitchell L. Moss - Urban Policy and Planning
Dr. Rae Zimmerman - Planning and Public Administration

Polytechnic Institute of NYU
Dr. Kaan Ozbay - Civil Engineering
Dr. John C. Falcocchio - Civil Engineering
Dr. Elena Prassas - Civil Engineering

Rensselaer Polytechnic Institute
Dr. José Holguín-Veras - Civil Engineering
Dr. William "Al" Wallace - Systems Engineering

Rochester Institute of Technology
Dr. James Winebrake - Science, Technology and Society/Public Policy
Dr. J. Scott Hawker - Software Engineering

Rowan University
Dr. Yusuf Mehta - Civil Engineering
Dr. Beena Sukumaran - Civil Engineering

State University of New York
Michael M. Fancher - Nanoscience
Dr. Catherine T. Lawson - City & Regional Planning
Dr. Adel W. Sadek - Transportation Systems Engineering
Dr. Shmuel Yahalom - Economics

Stevens Institute of Technology
Dr. Sophia Hassiotis - Civil Engineering
Dr. Thomas H. Wakeman III - Civil Engineering

Syracuse University
Dr. Riyad S. Aboutaha - Civil Engineering
Dr. O. Sam Salem - Construction Engineering and Management

The College of New Jersey
Dr. Thomas M. Brennan Jr - Civil Engineering

University of Puerto Rico - Mayagüez
Dr. Ismael Pagán-Trinidad - Civil Engineering
Dr. Didier M. Valdés-Díaz - Civil Engineering

UTRC Consortium Universities

The following universities/colleges are members of the UTRC consortium.

City University of New York (CUNY)
Clarkson University (Clarkson)
Columbia University (Columbia)
Cornell University (Cornell)
Hofstra University (Hofstra)
Manhattan College (MC)
New Jersey Institute of Technology (NJIT)
New York Institute of Technology (NYIT)
New York University (NYU)
Rensselaer Polytechnic Institute (RPI)
Rochester Institute of Technology (RIT)
Rowan University (Rowan)
State University of New York (SUNY)
Stevens Institute of Technology (Stevens)
Syracuse University (SU)
The College of New Jersey (TCNJ)
University of Puerto Rico - Mayagüez (UPRM)

UTRC Key Staff

Dr. Camille Kamga: *Director, Assistant Professor of Civil Engineering*

Dr. Robert E. Paaswell: *Director Emeritus of UTRC and Distin*guished Professor of Civil Engineering, The City College of New York

Herbert Levinson: *UTRC Icon Mentor, Transportation Consultant and Professor Emeritus of Transportation*

Dr. Ellen Thorson: *Senior Research Fellow, University Transportation Research Center*

Penny Eickemeyer: *Associate Director for Research, UTRC*

Dr. Alison Conway: *Associate Director for Education*

Nadia Aslam: *Assistant Director for Technology Transfer*

Nathalie Martinez: *Research Associate/Budget Analyst*

Tierra Fisher*: Office Assistant*

Bahman Moghimi*: Research Assistant; Ph.D. Student, Transportation Program*

Wei Hao*: Research Fellow*

Andriy Blagay: *Graphic Intern*

1. Report No.	2.Government Accession No.	3. Recipient's Catalog No.
4. Title and Subtitle Finite Element Simulation of Truck Impacts on Highway Bridge Piers		5. Report Date April 2016
		6. Performing Organization Code
7. Author(s) Anil K. Agrawal and Xiaochen Xu		8. Performing Organization Report No.
9. Performing Organization Name and Address The City College of New York Convent Ave @ W140th Street New York, NY 10031		10. Work Unit No.
		11. Contract or Grant No. 49111-09-22
12. Sponsoring Agency Name and Address US Department of Transportation Washington, DC		13. Type of Report and Period Covered Final Report
		14. Sponsoring Agency Code
15. Supplementary Notes		

16. Abstract

Recent studies show that the dynamic forces because of truck impacts may be significantly higher than the 600kips force recommended by the AASHTO. Hence, there is a need to carry out detailed investigations on vehicular-bridge collision for a reliable evaluation of an existing bridge subject to impact by trucks and design of new bridges with more redundancy for vehicular impacts. In this research, an extensive investigation on the impact of a three-span steel girder bridge with reinforced concrete piers by a medium weight truck running at different speeds has been carried out using finite element models of bridge and the truck in LS-DYNA. The performance of the critical highway bridge components during vehicle collision and the factors causing damage/failure of the typical bridge components have been identified.

17. Key Words	18. Distribution Statement
Vehicular Impacts on Bridge Piers, Truck Impacts, Bridge Impact, LSDYNA	

19. Security Classif (of this report)	20. Security Classif. (of this page)	21. No of Pages	22. Price
Unclassified	Unclassified	40	NA

Form DOT F 1700.7 (8-69)

Disclaimer

The contents of this report reflect the views of the authors, who are responsible for the facts and the accuracy of the information presented herein. The contents do not necessarily reflect the official views or policies of the UTRC or the Federal Highway Administration. This report does not constitute a standard, specification or regulation. This document is disseminated under the sponsorship of the Department of Transportation, University Transportation Centers Program, in the interest of information exchange. The U.S. Government assumes no liability for the contents or use thereof.

Table of Content

1. INTRODUCTION

Thousands of highway bridges throughout the United States have been constructed and put into public service during the past several decades. Because of the long service duration of these bridges compared to the design life-span, the safety concerns of existing bridges has become crucial in recent years. A recent study has reported that 503 bridges of various types failed during 1989 to 2000 in the United States. The age of these failed bridges ranged from one year to 157 years, with an average of 52.5 years. Moreover, domestic and international terrorist activities have heightened the concerns about the safety of various infrastructure systems, and highway bridges could be among the most vulnerable targets of potential terrorist attacks. On the other hand, some catastrophic collapses of bridge systems have occurred because of accidental collisions of heavy vehicles with bridge piers in the past, resulting in loss of life and the complete deconstruction of the impacted bridges. An example event of bridge failure under vehicular impact is shown in Figure 1.

Figure 1: Semi Tractor-Trailer Crash on FM 3041 Bridge over I-45, Corsicana TX on May 30, 2007

The principal factors affecting bridge failures can be categorized as deficiencies in design, detailing, construction, maintenance, use of materials and inadequate capacity to resist effects of external events. First five deficiencies can be included in the category of internal enabling reasons for bridge failures, whereas the external events are responsible for triggering causes of these failures. During past decades, bridge structures were generally designed to resist gravity, wind and earthquake loads. Relevant few bridge design specifications achieved significant success in ensuring the safety of the public highway bridge structures during these loads. However, a highway bridge is always expected to experience various extreme events during its lifetime. For most of the bridges designed 30 years ago, extreme events in general and even the seismic loads were not included in the design considerations. It has been observed that approximately 83% (420 occurrences) of all bridges failures (503 occurrences) from 1989 to 2000 have been caused by external events [Wardhana and Hadipriono, 2003]. Based on the analysis of recent bridge failures, four external events: Hydraulic, Overload, Collision and Earthquake have been identified to cause the most significant failures of highway bridges.

Hence, it is important to investigate unavoidable extreme loads that may almost suddenly lead to the collapse of bridge structures. Newly designed bridge structures crossing highway or railroad must be capable of resisting vehicular collision loads. Likewise, existing vulnerable bridge structures should be evaluated and retrofitted to improve their resistance against vehicular impacts.

2. LITERATURE REVIEW

2.1 Current Design Provisions for Vehicle Collision

In most design manuals, vehicular collision loads are included in the category of extreme event loads. In order to protect bridges during accidental collisions by heavy vehicles, the AASHTO LRFD (1998&2007) code provides design criteria to incorporate vehicle collision-loads in the design of piers. The design provision requires that unprotected structural elements that may be impacted bluntly by a vehicle or train should be designed to resist an equivalent static collision force of 600 kips, which is assumed to act in any direction in a horizontal plane, at a distance of 5.0 ft above ground level. This 600 kips force is based full scale truck impact test carried out by TTI, as described later. For an individual column shaft, the equivalent static load should be considered as a point load. These AASHTO specifications have a number of significant limitations, including: (1) the design collision force is not specified as a function of the design velocity of the adjacent roadway or the vehicle characteristics, (2) dynamic interaction between the colliding vehicle and the bridge structure is not recognized, and (3) there are no guidelines on how to design a vulnerable member to ensure that it will survive a severe impact.

With concerns about the vague statement of the AASHTO code, some State DOT have tried to define their own policies for the design of bridge substructures vulnerable to potential vehicular collisions. For instance, the Minnesota DOT guideline recommends specific design requirements based on redundancy since the redundancy of bridge piers increases with an increase in the number of piers. New York State DOT has developed a Collision Vulnerability Manual in 1996. In this manual, a detailed procedure has been presented to quantitatively evaluate collision vulnerability of superstructures and substructures of highway bridges under the hazard of vehicular impact. The procedure of classifying and rating for bridge collision vulnerability is clear and applicable. It is applicable to new bridges, existing bridges and bridges programmed for rehabilitation. However, the guideline is based on qualitative factors, rather than mechanics based simulations.

2.2 Experimental and Numerical Investigation of Impact Loads on Bridge Structures

Unfortunately, because of significant costs, logistics of conducting full-scale tests and size effects involved with small scale tests on concrete structures, information available on full scale impact tests on real bridge piers under the impact of moving ships or moving vehicles is very limited. Recently, two experimental tests on vehicular collision with infrastructure have been reported in the literature. An experimental study of anti-ram bollards (Concrete filled steel columns acting as barrier to vehicles) based on truck collision testing was conducted in Hunan University, China [Xiao and Liu (2009)]. The Test bollards were concrete-filled steel tube columns with outer diameter of 219 mm and height of 1300 mm. The thickness of steel

pipe was 20 mm, and C40 concrete was filled in the steel tube. There were 5 columns in these testing bollards with the interval distance of 1500mm as shown in Figure 2.

(a) Front view of anti-bollards

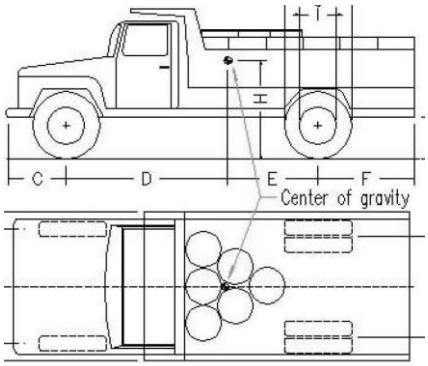

(b) Truck Geometry diagram

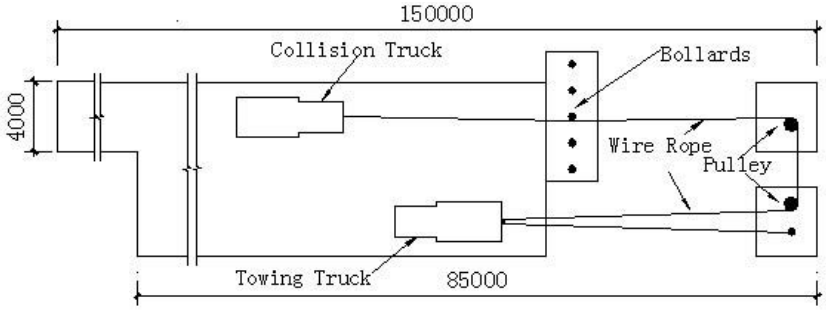

(c) Diagram of test site and facilities

(d) Truck and bollards after the collision

Figure 2: Truck collision Testing of Anti-ram Bollards

A Dongfeng EQ140 truck was selected as collision vehicle in the test shown in Figure 2(b). The weight of the truck was 5.17 tons and six petrol barrels filled with soil were loaded on the truck to reach the total weight of 6.8 tons. The collision test truck was driven by a wire system with a pulley wheel connecting the towing truck, as shown in Figure 2(c). The collision truck impacted the mid column with 40km/h (25.9 mph) speed. Figure 2(d) shows the truck and bollards after the collision. The acceleration time history of the moving truck was recorded during the impact test. The maximum acceleration was 52g and the associated maximum

impact force was measured as 3465KN (779kips). Considering 0.07 seconds of deceleration time, the average impact force of 1660 KN (373kips) has been calculated during the collision. Static load capacity of the bollard has been estimated as 350KN, which is about one fifth of the average impact force calculated based on the collision test. Because of the high capacity of the steel tube column filled with concrete, the column under impact didn't undergo large deformation and a residual displacement of only 33 mm was measured (a drift ratio of 2.54%).

Texas Transport Institute carried out experimental tests, sponsored by Federal Highway Administration, to study collision loads on bridge piers. The objective of these tests was to measure impact forces on the bridge piers. A 36-in diameter simulated steel bridge pier, 14 feet in height, was fabricated with 1 in thick A53 Grade B pipe material. The inner surface of the 36 in pipe was welded with a 120^{o} arch of A53 Grade B pipe (34-in in diameter and 1inch in thick). The steel pier was supported by braced column load frame and foundation system. The capacity of the test pier was extremely high and the pier could be considered as rigid body in the analysis. In addition to comprehensive accident survey and risk analysis of vehicle/bridge column and abutment collisions, two full-scale collision test involving 80,000lb heavy truck (2001 Freightliner FLD tractor and 1979 Bud van Trailer) were performed at TTI. The approach speed of the truck was set at 50 MPH in both cases. The difference in the two collision tests was the alignment of the truck with the pier. In the first test, right quarter point of the vehicle was aligned with the centerline of the pier, whereas the centerline of the vehicle was aligned with the centerline of the pier in the second test. The final images of first test are shown in Figure 3. In both these tests, there was no apparent structural damage in the rigid pier. Only cosmetic damage on the pier surface was observed. However, the vehicles suffered catastrophic damage.

(a) Test No.1 (b) Test No.2

Figure 3: Tractor-trailer and Rigid Steel Pier Collision Test by TTI.

The impact force was recorded by load cells installed at the top and bottom of the instrumented pier. Figure 4 shows impact force time histories for the two tests. It is observed from the time-history of the measurement that the peak impact force was 600 kips when the ballast hit the bridge in the first test. The peak impact force reached 900 kips in the second impact test because of the collision between the engine of the truck and the bridge pier. Based on the 900 kips impact forces, after several filtering processes, a value of 600 kips was taken as a more appropriate equivalent static force and was recommended to replace 400 kips force in the AASHTO guideline.

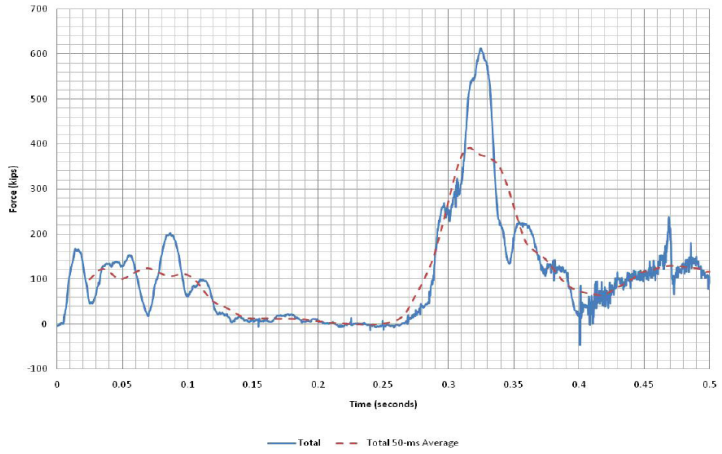

(a) Test No.1

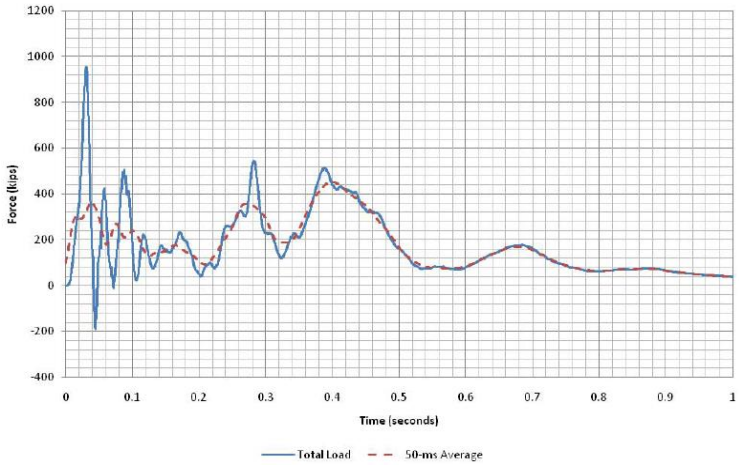

(b) Test No.2

Figure 4: Impact Force Time history recorded by TTI Test

The most recent published literature on vehicle collision simulation with bridge piers presents various data of interest which were extracted from the finite element results [EI-Tawil and Severino (2005)]. Two publicly available truck models were introduced in the simulation: a light weight truck with a weight of 14 KN and a medium weight truck with a weight of 66 KN. Two different bridge piers were studied and peak dynamic forces and equivalent static forces were calculated. Their results imply that the AASHTO-LRFD design provisions are not sufficient to protect bridge piers during reasonable crash scenarios. More research work on the simulation of vehicle bridge collision should be carried out to develop adequate design specifications. The peak impact force from the case of 66 KN (15,000 lb) truck with 90 KMH (56 MPH) speed reached the magnitude of 7600KN (1708kips), and even the related so-called ESF (equivalent static force) has been found to be 850 kips. Compared with 600 kips that the test result in the TTI study (80,000 lb truck with speed of 50 MPH), the 850 kips is extremely high, considering the fact that the weight of the truck is only one-fifth of that in the TTI test. Another major concern is the material models in the two studies cited above. The bridge pier in the research by Sherif (2005) was modeled with perfectly elastic material, whereas the pier

tested in the TTI study was very rigid without any deformation. It has been observed that the stiffness of bridge piers may influence the impact force between the pier and the truck.

3. OBJECTIVES OF THE RESEARCH

The objectives of this research work are to (i) develop high-fidelity finite element models of a typical highway bridge in USA, (ii) investigate the performance of the critical highway bridge components during vehicle collisions.

Develop and Validate a Reliable and High Resolution Finite Element Numerical Model: In order to simulate highly nonlinear bridge-vehicle impact problem, a reliable and high resolution full-scale finite element model of a 3-D bridge and a reliable finite element model of moving vehicles has been developed and validated. The element size, time step, material model and simulation time have been determined correctly to eliminate numerical errors and numerical instability. In this research, our focus is on a traditional concrete bridge substructure. Hence a reasonable concrete material model should represent realistic stress-strain relationship and damage modes of concrete under the specific strain rate according to the real physical mechanism. Reasonableness of the material model used in this research has been verified through comparison with available test results. In this research, LS-DYNA, which is one of the most investigated and well-developed hydro-codes, is used for the simulation of impact load effects on highway bridges.

Behavior of Bridge Components during a Vehicular Impact: There is very limited information on the behavior of bridge components and prominent failure modes during vehicular impacts. Using the 3-D finite element model of the bridge and the truck in LS-DYNA, extensive simulation have been carried out to investigate various failure modes of bridge components subject to vehicular impacts.

4. FINITE ELEMENT MODEL OF THE BRIDGE

In order to simulate localized failure modes of components of a bridge during vehicle impacts, a detailed modeling of all components representing actual bridge geometry is required so that all possible failure modes could be identified. In this research a finite element model of a three span bridge has been developed. Figure 5 shows a plan view and elevation of the typical bridge in this research. Table 1 shows key parameters of the bridge geometry and design load. This typical highway bridge is a three span non-continuous highway bridge with reinforced concrete piers and bents. The height of the pier is 16 ft. The length of middle span is 62 ft. The distance between the center lines of adjacent piers is 18 ft. Figure 6 shows rebar detailing in the piers and bent of the bridge.

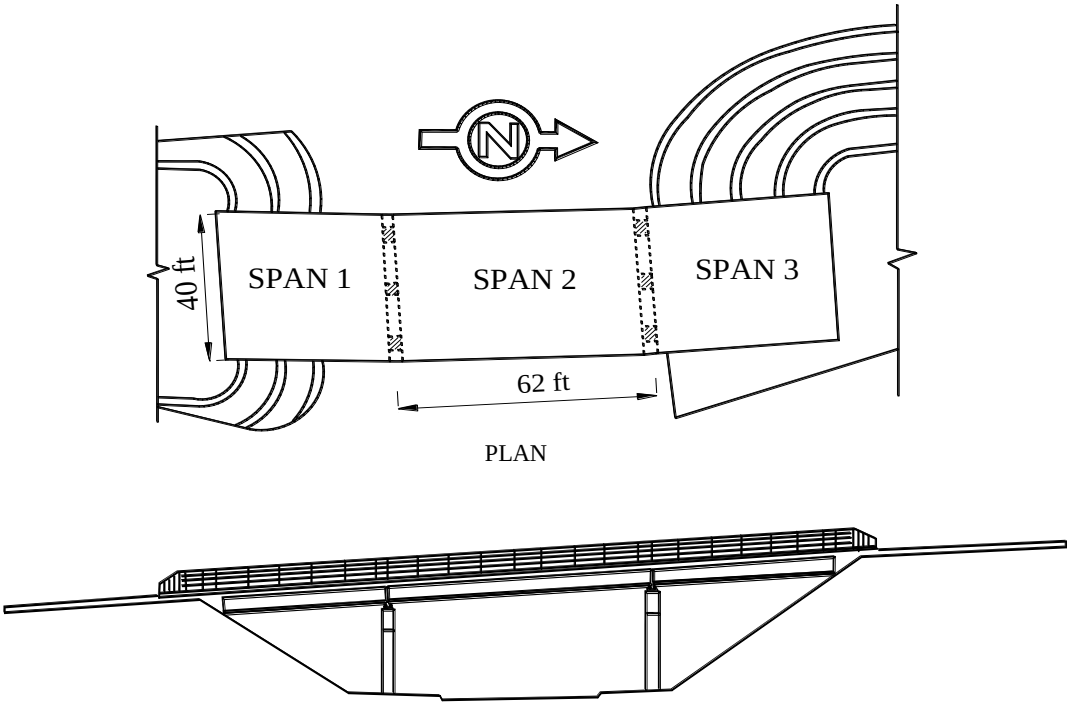

Figure 5: Plan View and Elevation of the typical bridge

Table 1: Key Parameters of the Bridge Geometry

ITEM	VALUE
Redundancy	Non-continuous
Length of Middle Span	62 ft
Number of Spans in Main Unit	3
Design Load	MS 18 or HS20
Deck Width	40 ft
Deck Thickness	13 in
Lanes on Structure	2
Height of Pier	16 ft
Number of Piers	3×(2bents)=6
Pier section	Rectangular 3.0ft×3.0ft
Material Type	RC concrete pier, bent &deck, steel stringer

The explicit solver in LS-DYNA has been selected for the simulation. The finite element model of the bridge is meshed with Lagrangian mesh, since constitutive equations can be easily applied on this kind of mesh and Lagrangian mesh is suitable for simulation of structures with large deformations. The element eroding technique is used to avoid severe element distortion during the simulation of the impact loads. In a step-by-step procedure of modeling by finite element methods, in order to investigate the behavior of each component of the bridge under

vehicle impact load, each component is built separately and assembled into a whole bridge in LS-DYNA preprocessor. Specifically, the footing, pier, bent bearing and deck are modeled by solid elements, stringers and diaphragms are modeled by shell elements and steel reinforcements are modeled by beam elements. Elastomeric bearings are used in this research since they are used extensively to replace old bearings. The characteristic mesh size of the concrete element is 1 in. The components of the bridge and related modeling elements are summarized in Table 2. Figure 7 shows the whole bridge finite element model.

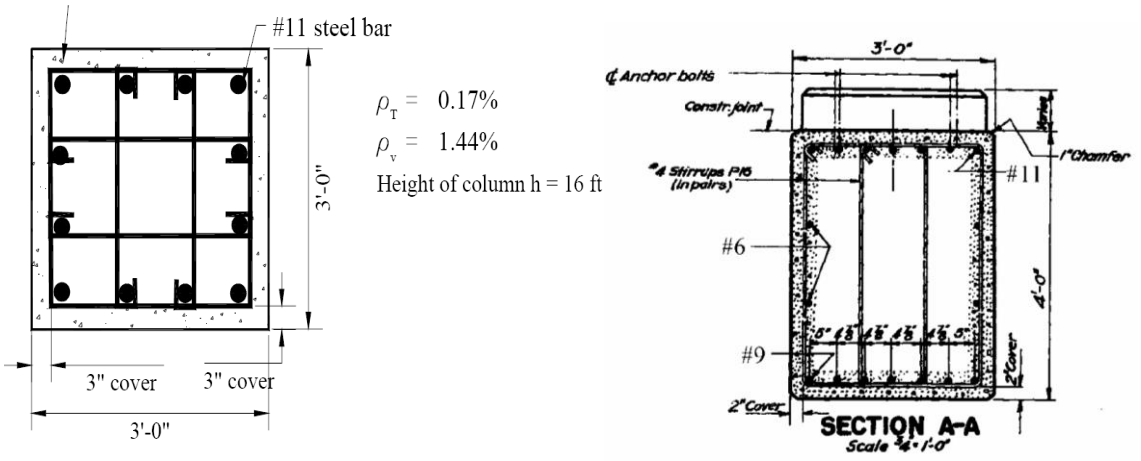

(a)Pier Section (b) Bent Section

Figure 6: Details of (a) Pier and (b) bent

Although superstructures of bridge are hit frequently by over height trucks, direct impact to pier by trucks usually causes serious damages, frequently leading to collapse of the entire bridge. The FEM model of the bridge pier consists of concrete core, cover concrete and steel rebar. According to Krauthmmer and Otani (1997), a detailed modeling of the rebars is important for the simulation of extreme loads on concrete structures. Generally, reinforced concrete members are modeled by an equivalent monolithic element that can represent combined behavior of both concrete and steel rebar during ordinary hazards such as seismic load, wind load, etc. However, monolithic element is not appropriate for reinforced concrete subject to vehicular impact loads. In this research, modeling of the reinforced concrete pier and bent is done by modeling concrete by pure concrete solid element and rebars as steel beam elements, which has been validated by the reinforced beam impact simulation in the previous section. For the geometry and rebar detailing given in Figure 6, Figure 8 shows finite element model of the pier.

Table 2: Element Types Used in the Bridge Modeling

Solid Elements	Footing, Piers, Bent, Deck, Concrete Support, Elastomer Bearing
Shell Elements	Stringers, Diaphragms
Beam Elements	Steel Reinforcements

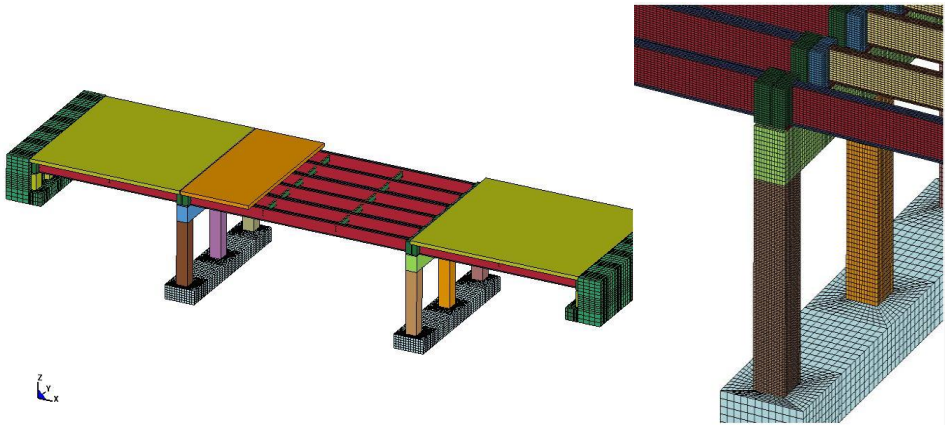

(a) Whole Bridge Model (b) Local Detailing of the Model

Figure 7: Finite Element Model of the Three-span Bridge

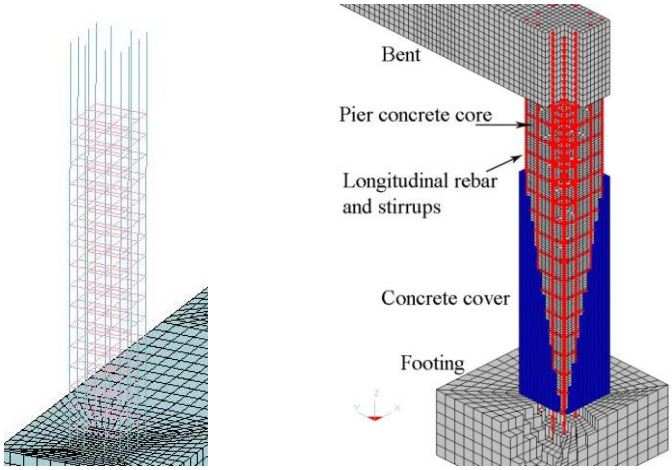

Figure 8: Modeling of Concrete Pier

In modeling of piers, core concrete and cover concrete are modeled as separate layers to include confining effects of steel rebars on core concrete. Rebar cage for concrete piers has been developed by modeling rebars with beam elements as shown in Figure 8. The longitudinal rebars have been extended into the footing and the bent as per as built bridge drawings. Core concrete is added to the rebar cage and cover concrete is added as a separate layer with different material properties on top of the core concrete. The detailed modeling of the bridge pier, pier-bent and footing, as shown in Figure 8, has been done so that failure mechanisms of the pier system subject to vehicle impact can be identified. It is mentioned that the footings of bridge piers are directly anchored to the bedrock.

5. VALIDATION OF CONCRETE MATERIAL MODEL

The research carried out in this report focuses on the numerical simulation of bridges impacted by trucks and investigates the structural response and failure mechanisms of highway

bridges using the explicit finite element method. The first and essential step in the simulation is to build a reliable high fidelity finite element model of the bridge and the vehicle with appropriate numerical algorithms and correct material models. The FEM vehicle models have been built and tested by the research center of the automobile industry. Based on several years of extensive work, vehicle FEM models have been revised and validated on the basis of experimental crash tests. Hence, the available truck model, which has been adopted in this research, is believed to be numerically stable and reliable.

In this section, we present a detailed approach for the modeling of highway bridges. The procedure of modeling a bridge by finite element method is shown in the Figure 9. In the numerical simulation using explicit finite element method, material properties, mesh size and time step size are important factors for ensuring reliable results. Furthermore, if the contact and erosion effects of the concrete material are considered in the simulation, the eroding contact algorithm and hourglass energy should still be carefully analyzed to ensure numerical stability and reliability of numerical results. The following parts of this section present detailed description of the modeling and validation of the concrete material model, numerical bridge model, and related numerical algorithm for the vehicle bridge collision simulation using LS-DYNA.

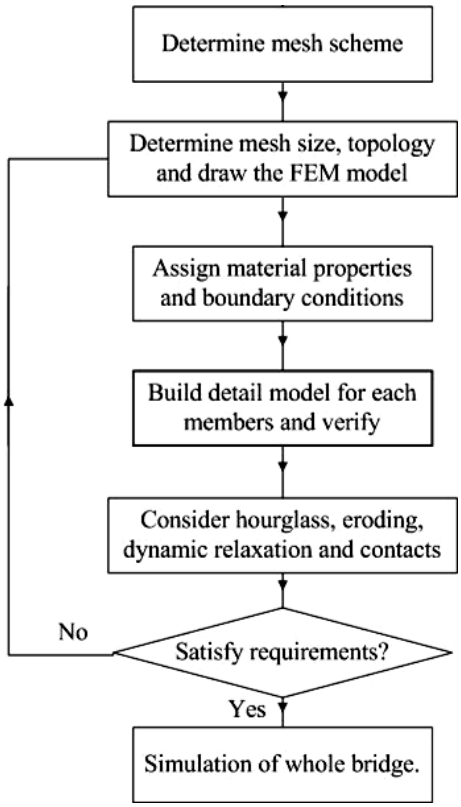

Figure 9: Procedure of FEM modeling of highway bridges

5.1 Concrete Material Model for Impact Loads

In the current version of LS-DYNA, there are five concrete constitutive models to simulate the behavior of concrete structures. Three concrete material models (Plastic/kinematic Model,

soil/Concrete Model and Winfrith concrete model) are not suitable for solving problems with damage failure, large strains and high strain rates. The remaining two concrete material models (Johnson-Cook Holmquist Concrete Model and Continuous Surface Cap Concrete Model) include material damage, strain rate effects and permanent damage erosion, which are highly nonlinear effects during high speed impacts. Even though these two models are mathematically complicated and require significantly higher level of computer capacity and time, they are much more reliable for identifying failure modes of concrete bridge piers subject to loads with high strain rates, such as blast and impact. In this section, we perform a comparison between these two models based on available examples.

5.1.1 Johnson Holmquist Cook Concrete Model

Holmquist and Johnson (1993) presented a computational constitutive model for concrete subjected to large strains, high strain rates and high pressure in the Fourth International Symposium on Ballistics. This constitutive model has been incorporated into LS-DYNA to simulate the concrete behavior under high speed impacts. This model is originally based on the Johnson Cook Model proposed to investigate fracture characteristics of three metals subjected to various strains, strain rates, temperature and pressures [Johnson and Cook (1983)]. It is first assumed that the difference between the "dynamic" material property and "static" material property is not only because of the strain rate effects, but also because of the large strains, high temperature and high pressure associated with high strain rates. The Johnson Cook Model for metals assesses the effects of each variable properly. A cumulative-damage fracture model has been developed and evaluated with an independent series of tests and computations.

In the JHC model, the normalized equivalent stress is defined as $\sigma^* = \sigma / f_c'$, where σ is the actual equivalent stress and $f_c^{'}$ is the quasi-static uniaxial compressive strength of the concrete. The normalized equivalent stress σ^* is expressed as:

$$\sigma^* = [A(1-D) + BP^{*N}][1 + C\ln\dot{\varepsilon}^*] \quad (1)$$

where D is the damage ($0 \le D \le 1$), in the same manner similar to that used in the Johnson-Cook Fracture Model for metals, which accumulates damage from an equivalent plastic strain; $\dot{\varepsilon}^* = \dot{\varepsilon} / \dot{\varepsilon}_0$ is the dimensionless strain rate (where $\dot{\varepsilon}$ is the actual strain rate and $\dot{\varepsilon}_0$ =1.0 S^{-1} is the reference strain rate); ***A*** is the normalized cohesive strength, *B* is the normalized pressure hardening coefficient and ***N*** is the pressure hardening coefficient. Using test data on perforation of concrete slabs having 48 MPa and 140 MPa unconfined compressive strengths [Hanchak (1991)], parameters for the JHC model in equation (1) can be determined using a procedure similar to that for Johson-Cook fracture model for metals. Even though there are 26 parameters for the JHC model in the material card of LS-DYNA, most of the parameters are not sensitive to variation in concrete strength and can be assumed to be the same as those provided by Holmquist and Johnson (1993). The specific description of the parameters for the JHC model can be found in the material manual of LS-DYNA for Model_111. Computational results using the JHC model show a good agreement with experimental results on penetration tests of concrete under impact of steel bullet obtained by Hanchak (1991).

5.1.2 CSCM Concrete Material Model

In order to improve roadway safety, the Federal Highway Administration (FHWA) sponsored a study by APTEK Incorporated and the Texas Transportation Institute to develop a concrete material model for use in roadside safety simulations, implement the model into LS-DYNA finite element code, and evaluate the model against available data. The concrete model developed by APTEK is referred to as a smooth or continuous surface "cap" model (CSCM).

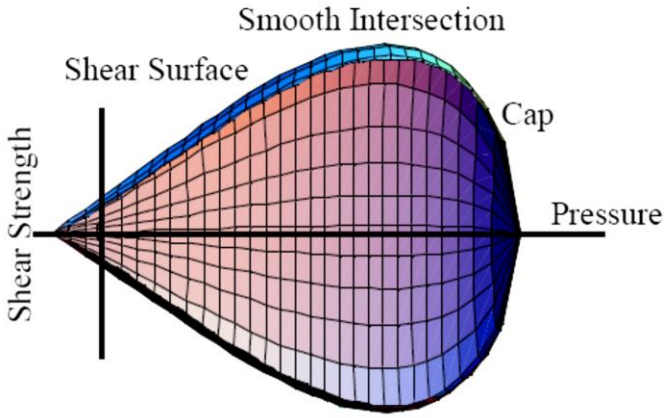

Figure 10: General shapes of the concrete model shear failure and cap hardening surfaces in two dimensions.

As shown in Figure 10, the failure surface is plotted as shear strength versus pressure, and a smooth and continuous intersection is formulated between the failure surface and hardening cap. The theoretical description of this concrete model contains constitutive equations, yield and hardening surfaces, damage-based softening with erosion and rate effects formulation for the increase of strength with strain rate. Used as a comprehensive material model for concrete, particularly for modeling strain softening in tensile and low confining pressure regimes, the model can be grouped into five formulations, which are elastic update, plastic update and yield surface definition, damage, rate effects, and kinematic hardening.

Elastic: Concrete is assumed to be isotropic and Hooke's Law is applied with two constants: the bulk modulus (**K**) and the shear modulus (**G**).

Plastic and Yield Surface: If a trail elastic stress σ_{ij}^{T} lies inside the yielding surface, the behavior is elastic, otherwise the behavior is elastoplastic with possible damage, hardening and rate effects, and plasticity algorithm returns stress state to the yield surface, and related elasto-plastic stress is denoted as σ_{ij}^{P} . The yielding surface uses a multiplicative formulation to combine shear (failure) surface with hardening compaction surface (cap) smoothly and continuously, which is referred to as smooth cap model, as shown in Figure 10. The yielding surface is formulated in terms of three invariants, J_1 -the first invariant of the stress tensor, $J_2^{'}$ -the second invariant of the deviatoric stress tensor, and $J_3^{'}$ -the third invariant of the deviatoric stress tensor. $J_1, J_2^{'}$ and $J_3^{'}$ are defined in terms of the deviatoric stress tensor S_{ij} and pressure P . The yield function is defined as

$$f(J_1, J_2^{'}, J_3^{'}, \kappa) = J_2^{'} - \Re^2 F_f^2 F_c \tag{2}$$

where κ is the cap hardening parameter; F_f is the shear failure surface, F_c is the hardening cap, and $\Re$ is the Rubin three-invariant reduction factor.

Shear Surface and Cap Hardening Surface: The strength of concrete is modeled by the combination of the cap and the shear surface in the low to high confining pressure regimes. The shear surface is defined along the compression meridian and the cap function has a tedious but straightforward definition which can be found in the LS-DYNA User Manual(2007). Figure 11 shows the failure surface combining the shear surface and the cap surface in one dimension for typical concrete values.

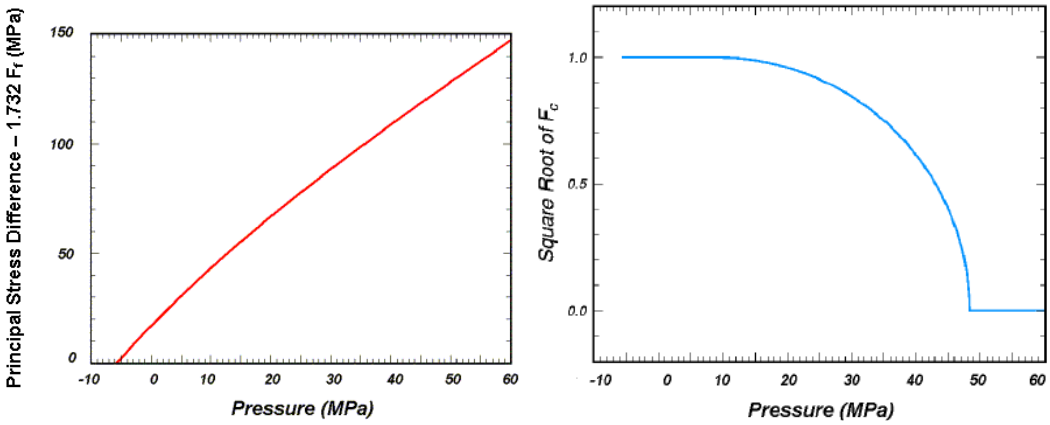

(a) Graph Schematic of Shear Surface (b) Graph Schematic of Cap Function

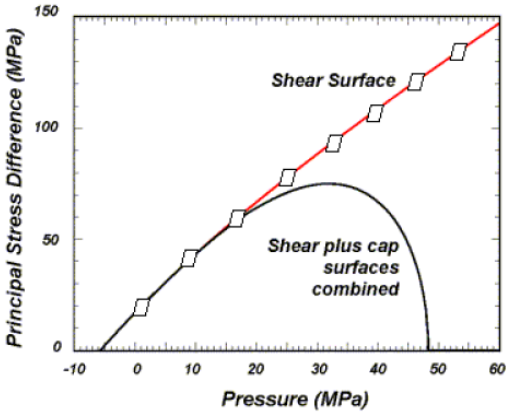

(c) Combined Failure Surface

Figure 11: Multiplicative Formulation of the Shear and Cap Surfaces

Damage: Damage accounts for the softening of concrete in the tensile and low to moderate compressive regimes. The damage formulation models both strain softening and modulus reduction. Strain softening is a decrease in strength during progressive straining after a peak strength value is reached; the modulus reduction is the reduction in the unloading/loading slopes in the process of cyclic unload/load tests. Damage initiates and accumulates when the strain-based energy terms exceed the threshold and is based on

two distinct formulations: brittle damage and ductile damage, where brittle damage accumulates when pressure is tensile and the ductile damage accumulates when pressure is compressive. Brittle damage accumulation depends on the maximum strain, $\varepsilon_{\max}$, which is defined as

$$\tau_b = \sqrt{E\varepsilon_{\max}} \tag{3}$$

Brittle damage initiates when τ_b exceeds an initial threshold. Ductile damage accumulation depends on the total strain components, ε_{ij}, which is defined as

$$\tau_d = \sqrt{\frac{1}{2}\sigma_{ij}\varepsilon_{ij}} \tag{4}$$

The stress components σ_{ij} are the elasto-plastic stresses calculated before application of damage and rate effects. Ductile damage initiates when τ_d exceeds an initial threshold.

Rate Effects: rate effects accounts for an increase in strength with increasing strain rate, and are applied to the plasticity surface, the damage surface and the fracture energy.

In order to evaluate the CSCM model, the model developer performed numerical simulations for basic material properties to reinforced concrete structures. These detailed studies include single element simulations to check the implementation of the model via examination of the stress versus displacement behavior; plain concrete cylinder simulation to check the damage modes; drop tower impact simulation and the bogie vehicle impact simulation of reinforced concrete compared with experimental data. All the work shows that that CSCM model can accurately simulate the displacement and damage modes of reinforced concrete structures under dynamic loading.

The current version of CSCM model in LS-DYNA has 37 input parameters. 19 parameters of the 37 input parameters must be fit to the data from triaxial extension (TXE) tests, triaxial compression (TXC) tests and torsion (TXO) tests. However, the usage of the model has been made easy by implementing a set of standardized material properties for use as default material properties. The CSCM model with default input parameters for normal strength concrete (with compressive strengths between 28MPa to 58MPa), and with aggregates sizes (between 8mm and 32mm) has been provided. Hence, concrete compression strength, aggregate size and unit of these parameters are the necessary input parameters for the CSCM material model in this report.

5.1.3 Single Material Cylinder Simulations

This section presents comparison between single material cylinder simulations using JHC and the CSCM models under different loading rates since the simulations of plain concrete allow us to evaluate the behavior of the concrete model without the complicated effects of steel reinforcement. The length of the concrete cylinder is 304.8mm (12 inches) and the diameter is 152.4mm (6 inches), as shown in Figure 12. The bottom of the steel end cap of the cylinder is fixed. The loading condition is an unconfined compression at the top of the steel end cap.

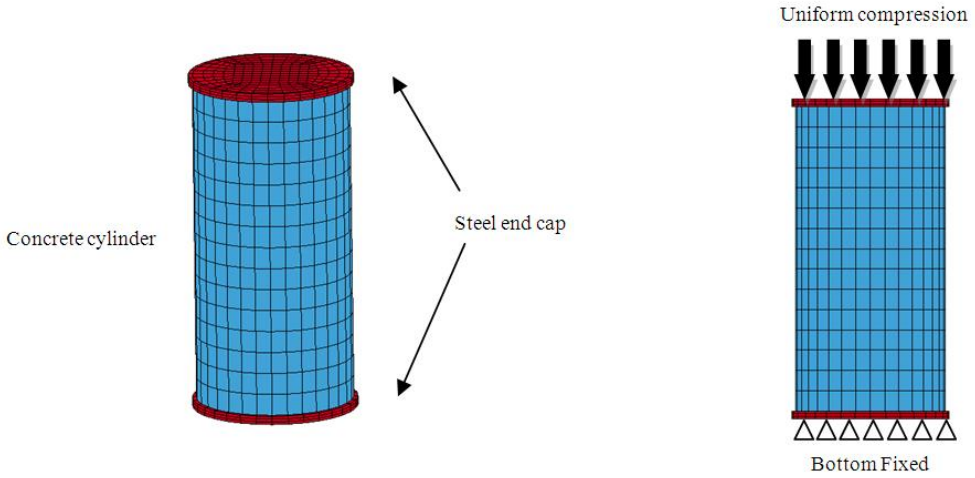

Figure 12: Numerical Model of Plain Concrete under Unconfined Compression

A uniform displacement was applied to the nodes at the top end cap. However, the loading time was varied, so this type of displacement control was expected to simulate the formation and failure modes of concrete cylinders with different loading strain rates. The mesh size of the concrete cylinder was taken as about 20 mm, which was recommended by the CSCM concrete model developer. The strength of the concrete was assumed as 46 MPA and the size of aggregate was set as 19 mm in the simulation. The cylinder was compressed by approximately 3.81 mm (0.15 in) during the loading durations of 1 ms, 10ms, 100ms, and 1000ms respectively. Figures 13-16 show the damage mode on a slice through the mid plane of the cylinder simulated using two concrete models under loading strain rates with durations 1000 ms, 100 ms, 10 ms and 1 ms, respectively. Fringe levels in these figures show the damage level calculated by the concrete model. A fringe value of 0 indicates no damage, whereas a value of 1 indicates maximum damage in which the stiffness and strength of concrete are reduced to zero. When a concrete element loses all strength and stiffness or the maximum principle strain is greater than a user-supplied input value, the element is eroded from the numerical model to prevent computational difficulties.

As the loading time is decreased from 1000 ms to 1 ms, which means the loading strain rates increases 1000 times, the damage mode of the cylinder modeled with JHC model doesn't change significantly. On the other hand, the damage mode of the cylinder using the CSCM model varies with the loading strain rate. In Figure 13, where the loading time is 1000 ms (which is almost close to quasi-static loading), the damage mode of the cylinder using CSCM model matched well with the concrete cylinder test shown in Figure 17, since an obvious shear failure appeared in the cylinder. In the case of 1 ms loading time, Figure 16 shows that the damage mode (in the middle of the cylinder) of the cylinder using CSCM model matches with that using the JHC model. This implies that the CSCM model can simulate the same damage mode as that by the JHC model when the strain rate is high.

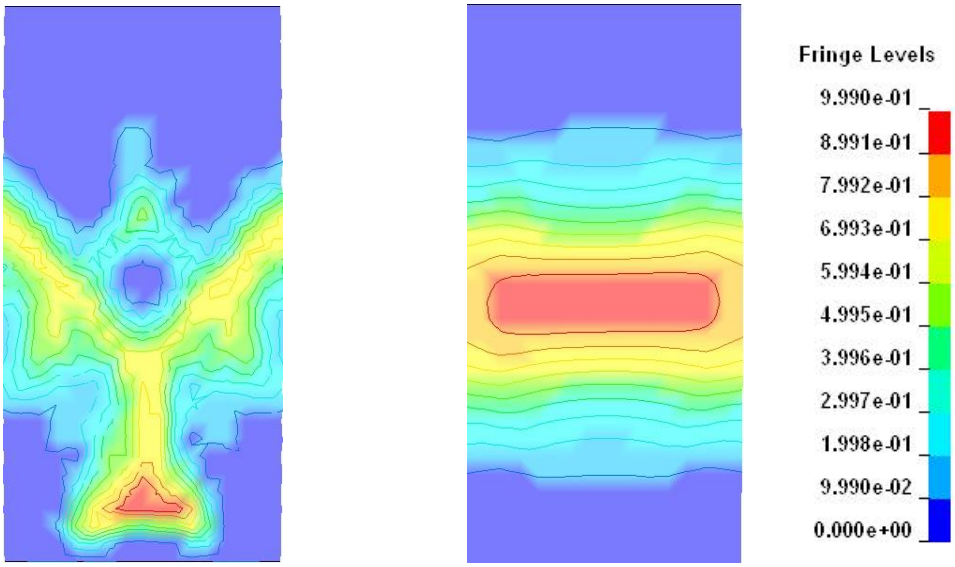

(a) CSCM Model (b) JHC Model (c) Damage Level

Figure 13: Damage Mode of Cylinder with Loading Time of 1000ms.

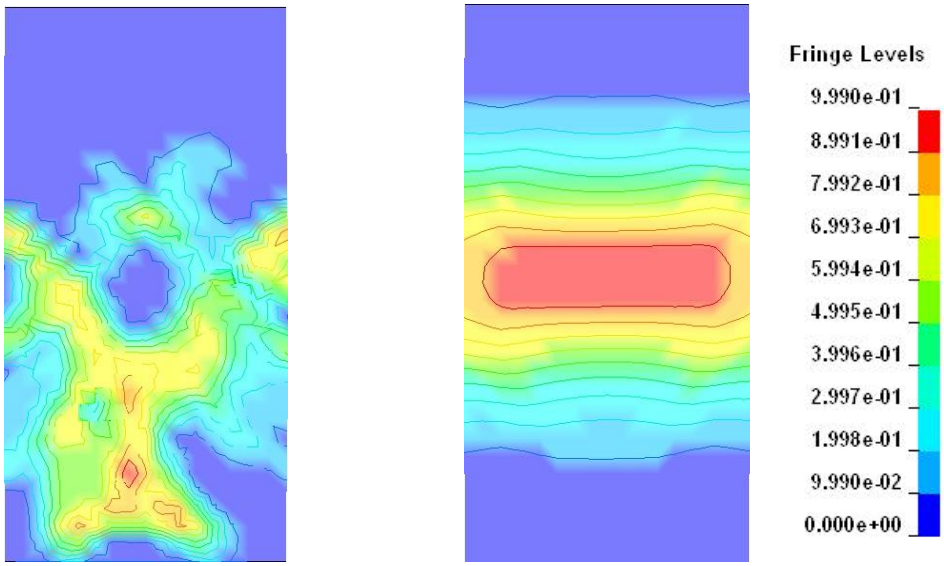

(a) CSCM Model (b) JHC Model (c) Damage Level

Figure 14: Damage Mode of Cylinder with Loading Time of 100 ms.

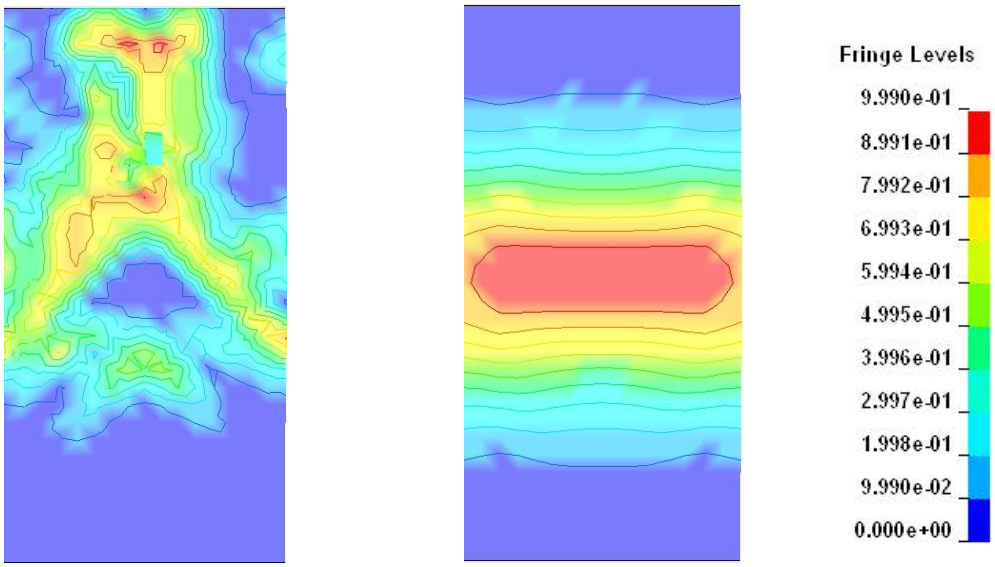

(a) CSCM Model (b) JHC Model (c) Damage Level

Figure 15: Damage mode of Cylinder with Loading Time of 10 ms.

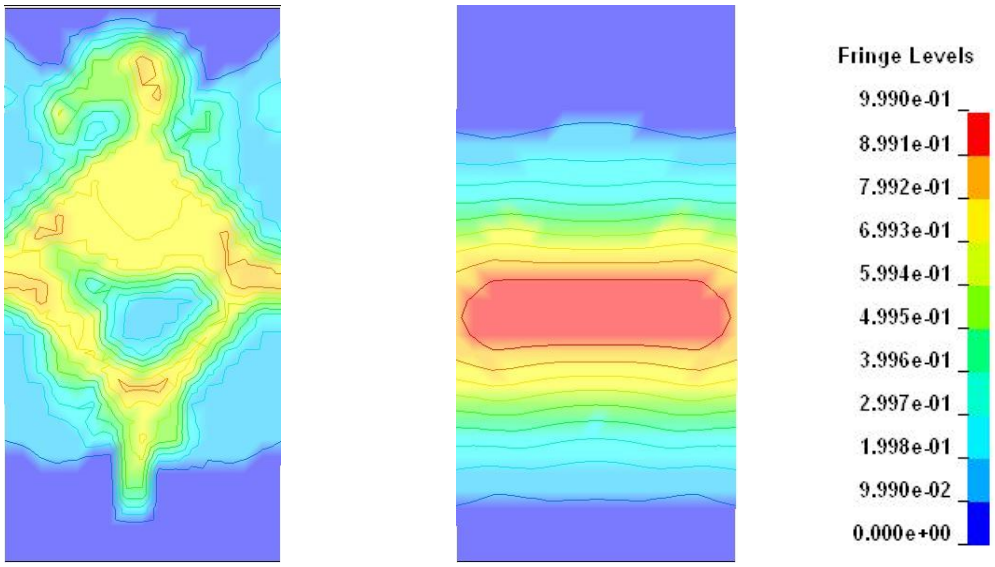

(a) CSCM Model (b) JHC Model (c) Damage Level

Figure 16: Damage mode of Cylinder with Loading Time of 1 ms.

It has been noted that the JHC model for concrete is typically based on the same mathematical plasticity theory used to model common metals. However, the constitutive behavior of concrete differs from that of metals. Concrete displays brittle behavior in tension and its compressive strength is almost ten times its tensile strength. The yield stress depends on the mean stress (pressure). Hence, it can be concluded from these observations that the JHC model cannot appropriately simulate the concrete behavior in low to medium range of strain rates. For very high strain rate cases with high confined pressure, such as the cases of

high speed penetration and explosive blast loading, JHC model is preferred. The JHC model also improves convergence and reduces computational time in such cases because of its comparably simpler mathematical expression. The impact speed of the vehicle during impact with bridges is significantly lower than those for blast and flying missile cases. Loading strain rates during vehicular impact cases are not in the applicable region of the JHC model. Hence, the CSCM model has been used in this report to simulate the dynamic behavior of the concrete structures.

Figure 17: Concrete Cylinder Compression Test under Quasi-static Load.

5.2 Numerical Algorithm for the Finite Element Analysis

The validation of the numerical model should be discussed based on the mesh size sensitivity and integration time step because the finite element method solves partial differential equations through the discretization in space and time. Gebbekin and Ruppert (1999) state that "every finite method has methodical inherent errors of discretization in space (e.g. mesh size sensitivity) and in time (timestep)." The convergence theorem states that the numerical solution of a partial differential equation, which is discretized by finite elements method, must monotonically converge to the exact solution when element size and time step tend to zero.

5.2.1 Mesh size

Generally, a proper mesh size for a finite element problem is decided by convergence. If the difference in response using two different mesh sizes is small, the coarser mesh size is selected. For the finite element analysis of dynamic behavior of concrete structures, numerous previous studies discuss element size sensitivity. For the elastic response of a structure with homogeneous material, exact solution can be obtained by decreasing the size of the mesh to zero. However, this doesn't apply in the case of the inelastic response of structures with non-homogeneous material. In the case of concrete, cement is a porous material with low stiffness and highly compressible property, whereas the aggregate is very stiff and incompressible. If the size of the mesh is taken to be less than dimension of the aggregate, numerical results on failure modes in the structures may not be realistc, since fracture properties change dramatically. For commonly used concrete, crack always starts and moves along the cement

and doesn't propagate through aggregates. Bazant(2002) has shown that there exists a characteristic length for concrete material fracture.

However, the material model of concrete has to consider it as a kind of homogeneous material to avoid unsolvable complexity. Numerical modeling of the bond-slip problem in reinforced concrete should also be considered while determining the mesh size effect, since concrete and steel are modeled separately in one component of the bridge. Research on the influence of bond slip [Chen and Baker (2003)] shows that the damage near reinforcement is distributed when bond slip isn't considered in the modeling and it is localized when bond slip is considered. The bond between concrete and steel is highly nonlinear and can be matched with element size. Yi and Agrawal(2008) investigated effects of mesh size on the response on reinforced concrete members subjected to blast loads. Using four different element sizes to mesh a beam under blast loads and calibrating their numerical results with experimental tests carried out by Magnusson and Hallgren(2004), they found that the finite element model with a mesh size of 1.08 in matched the experimental results very well. In order to evaluate the CSCM model, the developer of the model conducted reinforced concrete beam drop tower impact simulations and impact tests on the safety-shaped barrier test. During the numerical simulations of their experimental results, they used solid elements of 1 inch length and verified the validity of the results. In this report, mesh size of the concrete element is taken as 1 inch for components directly affected by the impact load.

5.2.2 Time Step Size

For dynamic impact problems, a critical time step size should satisfy the following equation:

$$\Delta t_{crit} \leq \min_{e} \frac{l_e}{c_e} \tag{5}$$

where l_e is the smallest distance between any two nodes of an element and c_e is the instantaneous wave speed. Physically, this equation implies that the stress wave should not propagate further than the shortest length of one element in each time step to guarantee numerical stability. The critical time step is deduced from linear or linearized physically stable systems. Very little is known about the stability behavior of numerical procedures during physically unstable processes. Furthermore, the deduction of time steps considers only numerical stability (i.e., material stability is not considered). Generally, the smallest distance between two nodes is 1 in (mesh size) and the instantaneous wave speed can be taken as 10,000 in/s (2.5km/s) [Popovis and Song, (1998)]. Hence, Δt_{crit} should be 10^{-4} seconds. We can assume that numerical methods which are stable for linear systems are also stable for nonlinear systems. Hence, in this research, the time step is set as 1 μs (10^{-6} second).

5.2.3 Hourglass Effects and Energy Conservation

In order to avoid a numerical problem called "hourglass" because of one-point integration [Hallquist (1998)], a small damping is usually added into the system in the simulation of high strain rate problems by the explicit method. Undesirable hourglass modes tend to have periods that are typically shorter than the periods of structural response, and they are often observed to be oscillatory. Hourglass technique helps in avoiding all numerical stability problems caused

by zero energy modes, which means the explicit method with small damping is not suitable to study buckling problems for structures under high strain rate loads. The hourglass energy could be recorded during the simulation. In the head-on collision validation exercise conducted by Zaouk (1996), hourglass energy was reported as 17 % of the total energy. The total energy, kinetic energy, internal energy, energy loss due to element erosions and hourglass energy were recorded during the simulation. The evolution of various energy quantities are shown in Figure 18.

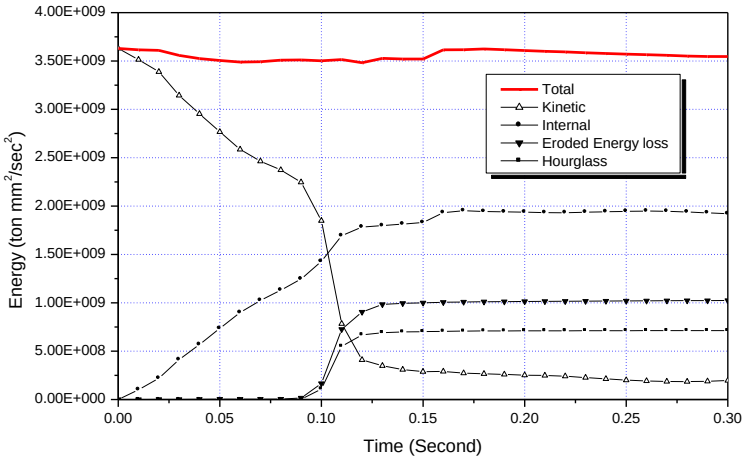

Figure 18: Time Histories of Various Energy Quantities for NY-70 Case

During vehicle impact to the bridge, kinetic energy of the vehicle is converted to target bridge's internal energy and internal energy of components of the vehicle itself. As the impact occurs, the kinetic energy of the vehicle gradually decreases as the internal energies of the target bridge and vehicle increase. The maximum energy exchange occurs at the time of 0.11 second, when heaviest carriage part of the truck hits the bridge pier. At this instant, 10% of energy accounting for erosion increases suddenly, since most of the eroded elements are deleted from the system. Finally, the hourglass energy takes 17% of the total energy whereas 25% energy is lost due to failure and erosion of elements during the vehicular impact. The final internal energy of the damaged bridge and the vehicle is almost 60% of the total energy of the whole system. However, the total energy keeps constant during the simulation, and conservation of the energy during the numerical simulation demonstrates numerical stability of the simulation.

5.2.4 Simulation of Reinforced Beams under Impact Loads

Because of the involvement of highly nonlinear damage mode in the simulation of vehicular impact loads on highway bridge piers, calibration of finite element model parameters, such as simulation time step, mesh size and material parameters with observed or experimental data is required. However, direct impact test data on reinforced concrete piers are not available in the literature. The calibration of the numerical model can only be carried out by using test data on reinforced concrete components made of similar material types. We try to employ this process to validate the parameters of material model, finite element mesh size, simulation time step and contact algorithm. We couldn't find any data on experimental tests on reinforced concrete columns (including reduced scale models) under impact load in the literature. On the other hand, numerous references are available on experimental tests on

reinforced concrete beams. For example, Krishis and Nakano (2001) conducted an experimental study on the ultimate strength of flexural-failure-type RC beams under impact loading. Eight 2-meters-clear-span RC beams of various cross sections and reinforcement ratios have been impacted by a 200 kg steel weight for various falling height. The impact force and the mid-span displacement have been recorded during the falling weight impact. Interesting findings in this research [Krishis and Nkano (2001)] include: (i) the maximum reaction force for all RC beams exceeds 2.0 times the corresponding reaction force during static bending, and (ii) the ratio of absorbed energy (estimated using the area of reaction force-displacement curve) to input kinetic energy are distributed in the region from 0.5 to 0.9 for all the tested RC beams (the mean value is 0.7). Based on these results, they assume the dynamic response ratio as 2.0 and the ratio of absorbed energy to input energy as 0.7 for all the cases of flexural-failure-type RC beams under impact loads. Although these results may not be applicable to the present research directly, they do serve as a meaningful basis to discuss the numerical results.

Most recent experimental tests to study the impact response of reinforced concrete beams have been carried out by Fujikake and Li (2009). They used a drop hammer with a mass of 400 kg to impact reinforced concrete beams. The influence of drop height and the effect of the longitudinal reinforcement ratio have been investigated. The RC beams specimens in their tests have cross-sectional dimensions of 250 mm in depth, 150 mm in width and 1700 in length, as shown in Figure 19.

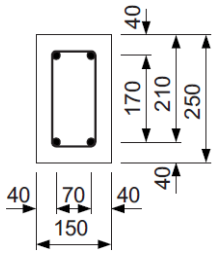

(a) Cross section View

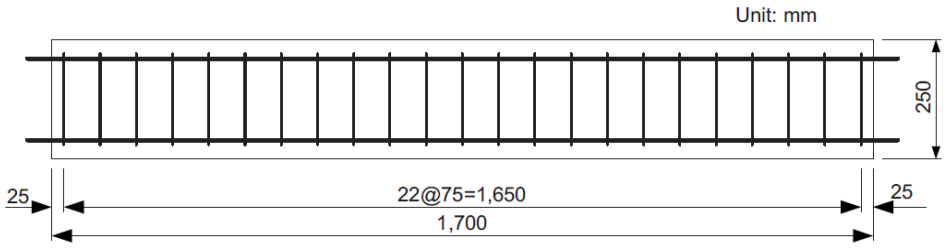

(b) Side view

Figure 19: Geometry and Rebar Detailing of the RC Beam Specimens

The RC beams specimens have been constructed using three longitudinal reinforcement ratios using D13, D16 and D22 deformed bars. The yield strength of D13, D16 and D22 bars are 397 MPa, 426 MPa and 418 MPa respectively. D10 bars with yield strength of 295 MPa have been used for stirrups. For each arrangement of longitudinal reinforcement, four impact

tests have been carried out by freely dropping a hammer of 400kg on the top surface of a RC beam (at mid-span) from four different heights. A total of 12 RC beams were tested under hammer impact loading. Table 3 presents the reinforcement arrangement for the RC beam specimens.

Table 3: Longitudinal Reinforcement Arrangement

	Compression side		Tension side	
Designation	Number and size (mm)	Area A_s (mm^2)	Number and size (mm)	Area A_s (mm^2)
S1616	2-D16	397	2-D16	397
S1322	2-D13	126.7	2-D22	774
S2222	2-D22	774	2-D22	774

The drop hammer impact test setup is shown in Figure 20. For beam series S1616, the hammer was dropped freely from four different heights of 0.15m, 0.3m, 0.6m and 1.2m. For beam series S1322 and S2222, the hammer was dropped from four different heights of 0.3m, 0.6m, 1.2m and 2.4m. The hammer had the hemispherical striking head with a radius of 90mm. The RC beam was supported by a device designed to allow it to freely rotate while preventing it from moving up or down. The span between the supports was set at 1400mm. The contact force between the hammer and the RC beam was recorded by the load cell attached with the hammer. The mid-span displacement was tested by a laser sensor. The strength of the concrete was 42 MPa and the maximum size of the aggregate was 10mm.

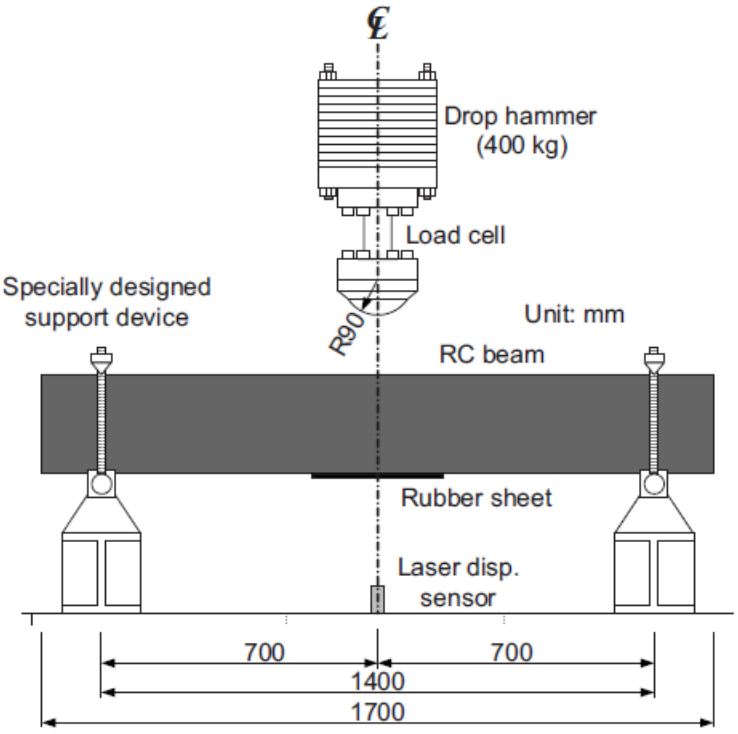

Figure 20: RC Beam Hammer Impact Test Setup.

It is observed from Table 3 that specimens in series S1616 and 2222 have the same longitudinal rebars on both tension and compression sides, which is similar to rebar detailing in columns. Hence, these two specimens have been selected for simulation in LS-DYNA. For series S1616 beams, tests with drop heights of 0.6m and 1.2m have been simulated. For series S2222, tests with drop heights of 1.2 m and 2.4m have been simulated. Table 4 summarizes bending and shear resistances for simulated beams.

Table 4: Numerical Simulation Cases for Beam Impact.

	Drop Height (m)	Bending resistance *RM*=4Mu/L (KN)	Shear resistance *RS*=2Vu (KN)	Shear to Bending ratio (*RS*/*RM*)
S1616	0.6	91.1	232.0	2.55
S1616	1.2	91.1	232.0	2.55
S2222	12.	162.6	245.4	1.51
S2222	2.4	162.6	245.4	1.51

Numerical models of impacts on RC beams have been built in LS-DYNA, as shown in Figure 21. Concrete components of the RC beam are modeled with eight-node solid elements with a characteristic size of 20mm. Steel Reinforcements are modeled by beam elements. Both solid and beam elements are meshed with the same size, so that the nodes of the concrete solid element could be attached to the nodes of beam elements to simulate the confinement of reinforcements. CSCM model is used to model material behavior of concrete. Main parameters of concrete in this model are the compressive strength of 42 MPa and aggregate size of 10 mm. Plastic-kinematic material model is used to the model beam elements with the same yield strength and plastic characteristics as the reinforcements in the impact tests. The elastic and hardening modulus of the reinforcement are taken as 200GPa and 3 GPa, respectively. The hamper is simplified into a half-sphere with a mass of 400kg, which is achieved by increasing the density in the material property definition. The half-sphere hammer was assigned an impact velocity calculated from different dropping heights. The hammer hit contacts and interacts with the top surface of the mid-span of the RC beam to simulate the impact loading. The time step is set as 10^{-6} second for each of the four cases.

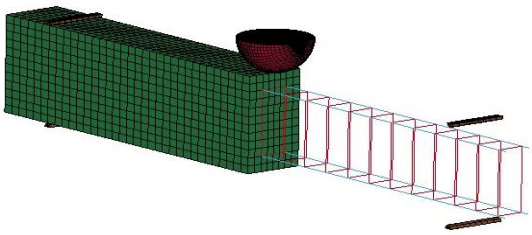

Figure 21: Numerical Model of the Beam Impact Test

Contact forces during the impact of the hammer on RC beams and displacements at the bottom surface of RC beams have been recorded in the simulation. The impact force time history and mid-span displacement time history plots are shown in Figures 22 and 23 for series S1616 beams. Figures 24 and 25 show these plots for series S2222 beams. In these figures, impact forces and displacement profiles measured during experimental tests by Fujikake and Li (2009) are also plotted for comparison.

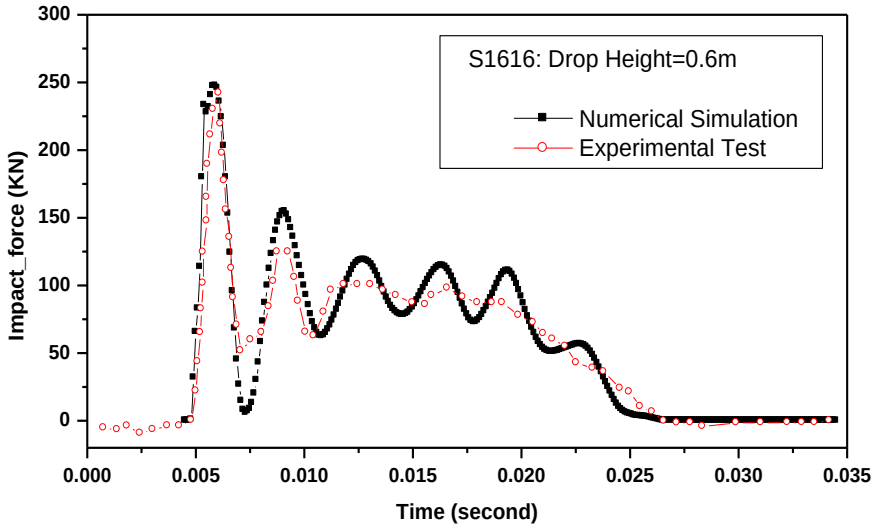

(a) Impact Forces Time History

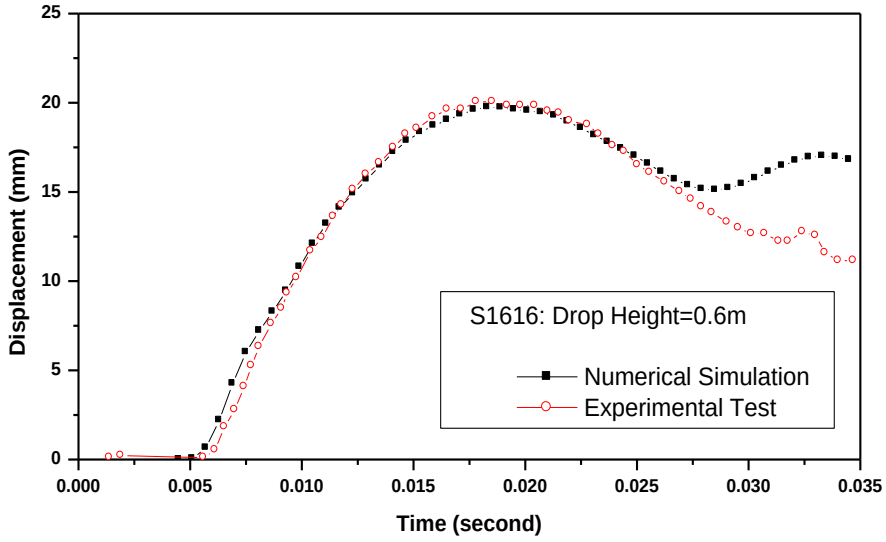

(b) Mid-span Displacement Time History

Figure 22: Impact Response Comparisons for S1616 with Drop Height of 0.6m.

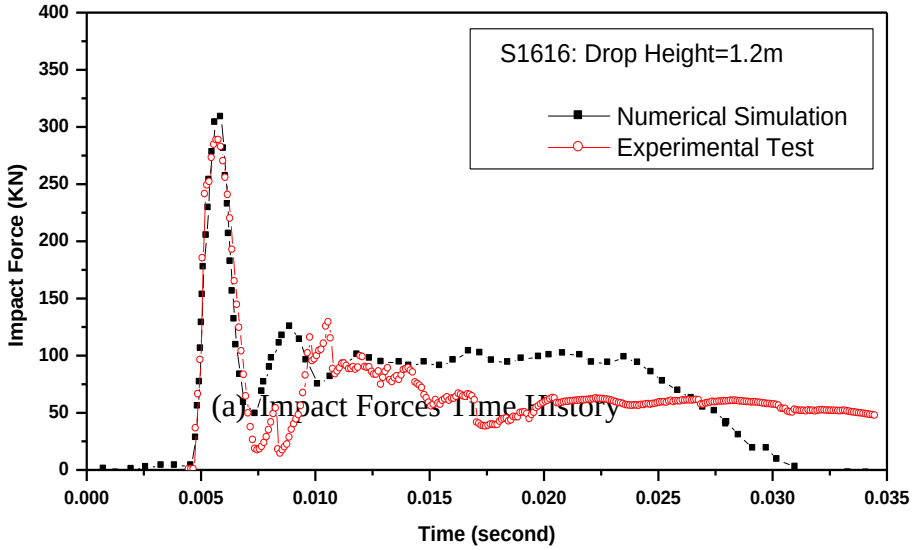

(a) Impact Forces Time History

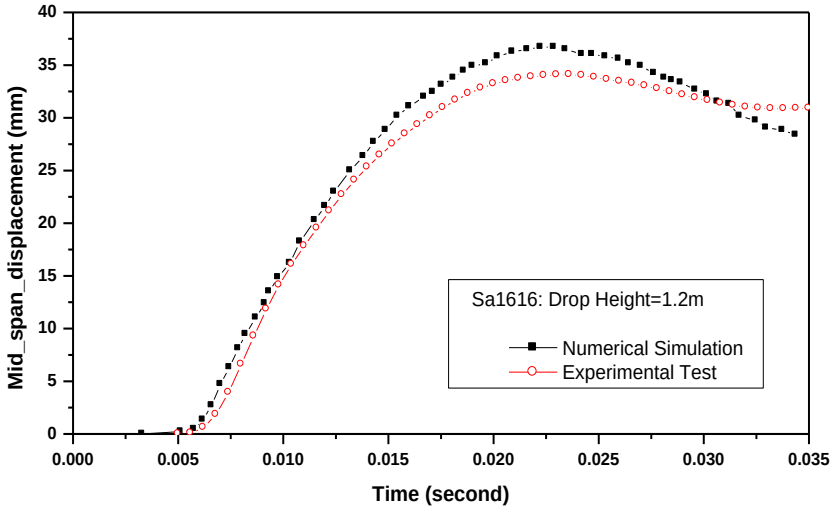

(b) Mid-span Displacement Time History

Figure 23: Impact Response Comparisons for S1616 with Drop Height of 1.2m.

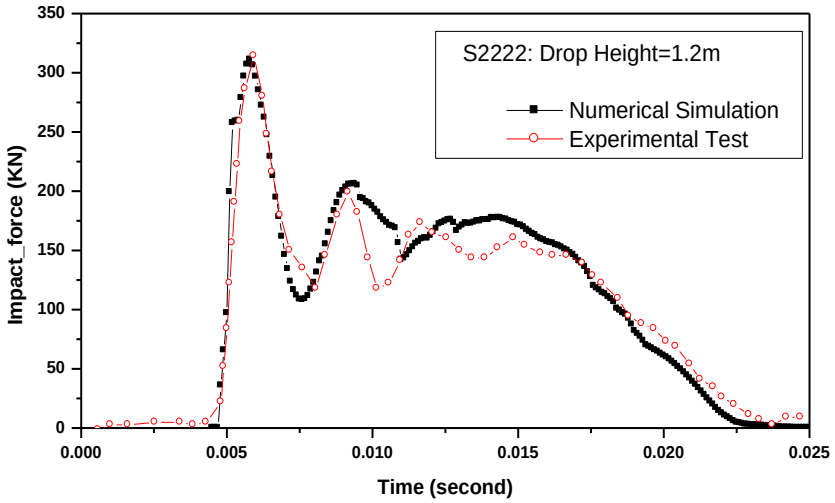

(a) Impact Forces Time History

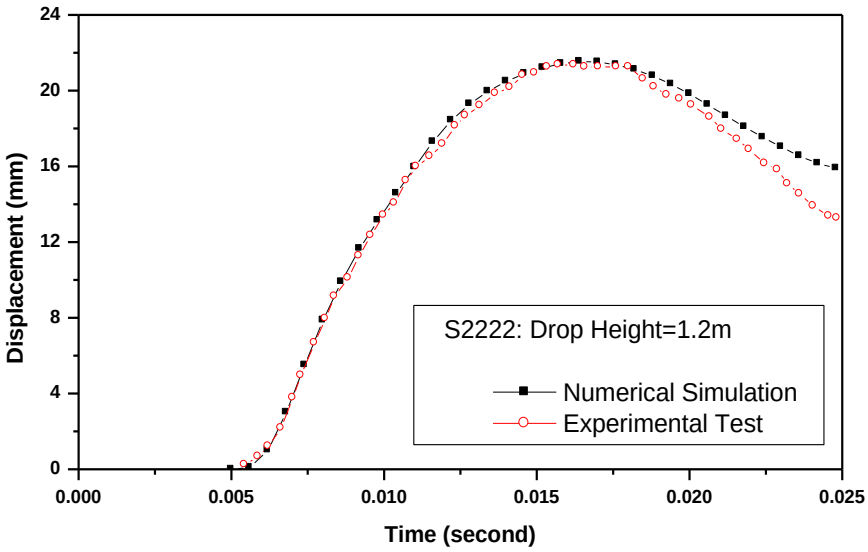

(b) Mid-span Displacement Time History

Figure 24: Impact Response Comparisons for S2222 with Drop Height of 1.2m.

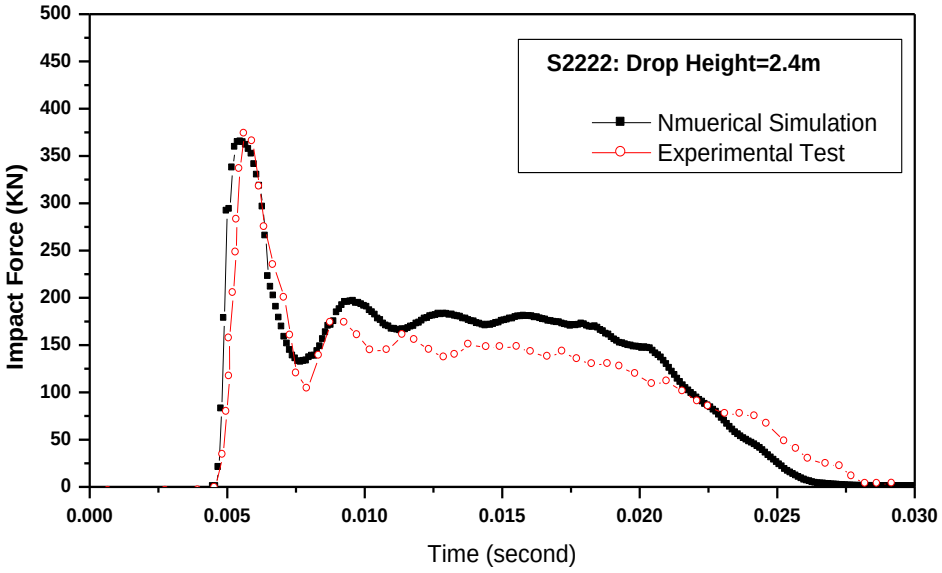

(a) Impact Forces Time History

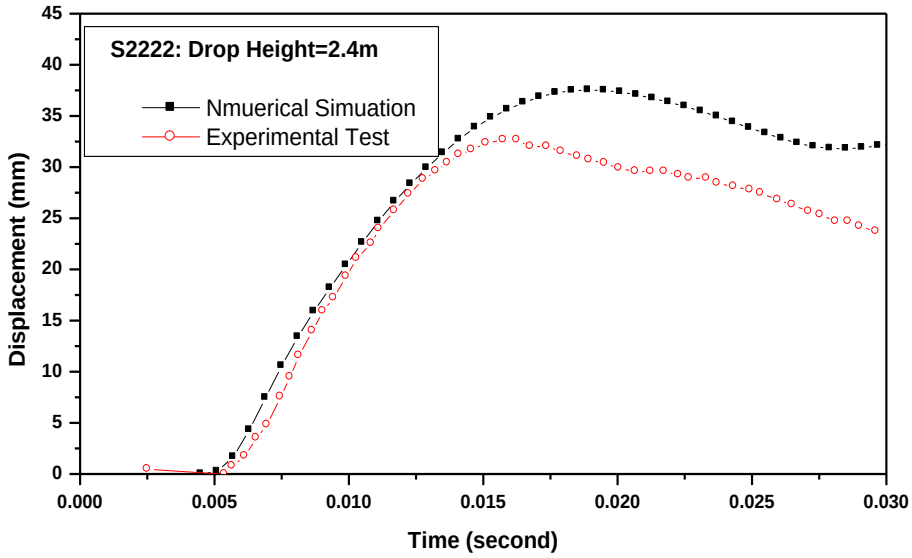

(b) Mid-span Displacement Time History

Figure 25: Impact Response Comparisons for S2222 with Drop Height of 2.4m.

It is observed from Figures 22 to 25 that both impact force and mid-span displacement profiles from numerical simulations match those from experimental tests very well. The displacement profiles from numerical simulations match those from experimental tests better for beams with lower longitudinal reinforcements and lower impact heights (Figure 22 to 23).

Reinforce concrete beams with higher longitudinal reinforcements are expected to display more local damage other than overall failure response. In cases with more local damages, numerical simulations overestimated the mid-span displacement as compared with experimental tests. However, the difference is still tolerable since the deviation of the two displacement results is within the range of 30%. The maximum impact forces from simulations match very well with those from the experimental tests. Since the geometry of beam supports and drop hammer are simplified in the simulation, the dynamic characteristics of the numerical model are different than those of experimental models. This results in lesser matching between numerical and experimental time-histories of impact forces at times after the peak impact force. This is more prominent in case of lower drop heights, e.g., Series S1616 beam with 0.6 m drop height, see Figure 22(a).

The simulations of RC beams impact are shown to be in good agreement with the experimental tests when RC beams exhibits a flexural failure, which could be taken as a calibration for the selection of material model, mesh size and time step to model the reinforced concrete components of highway bridges in this report. In the next section of this chapter, a three span highway bridge with concrete components will be built with the same material models and numerical algorithms as the RC beam specimens described in this section.

6. NUMERICAL SIMULATIONS OF VEHICULAR IMPACTS ON BRIDGE PIERS

The development of the design criteria for highway bridges, susceptible to vehicular impacts, depends on risk acceptance criteria, factors influencing the probability of vehicular impacts, failure modes of bridge components, and consequences of impacts. The risk acceptance criteria and factors influencing the probability have been discussed in various published guidelines. However, there is still a severe knowledge gap on determining the dominant failure modes and severity of collision in determining consequences. Generally, failure modes of highway bridges during vehicular collision are directly influenced by two main factors: characteristics of the truck (including its weight and velocity before a collision) and the design capacity of bridge piers. Traditionally, bridge piers are designed for dead, live and seismic loads, where lateral load capacity, rebar detailing and the size of piers are influenced or governed by seismic loads. Hence, it is important to investigate the influence of various levels of seismic detailing on damage and failure modes of bridge piers during vehicular impacts. A hypothetical bridge based on an existing bridge in the New York State is adopted in this research, and impacted by a medium weight truck with low, medium and high approach velocities to identify failure modes and damage scenarios. Table 5 shows the geometry and reinforcements arrangements for the New York Bridge.

A Ford Truck, which represents the medium weight truck model, has been built and evaluated by the National Crash Center at the George Washington University has been adopted in this research to impact the bridge pier. The weight of the truck is 15,000 pounds (66-KN), and the dimension of the truck model is 27 feet in length, 8 feet in width and 10 feet in height, as shown in Figure 26.

Table 5: Geometry and Reinforcement Arrangement of Piers in the Example Bridge

	Acceleration (g)	Pier Height (ft)	Pier Size (ft)	Longitudinal Bars	Stirrups Bars
NY Bridge	0.15	16	3	Bar 11 4×4	Bar 3 12 in Spacing

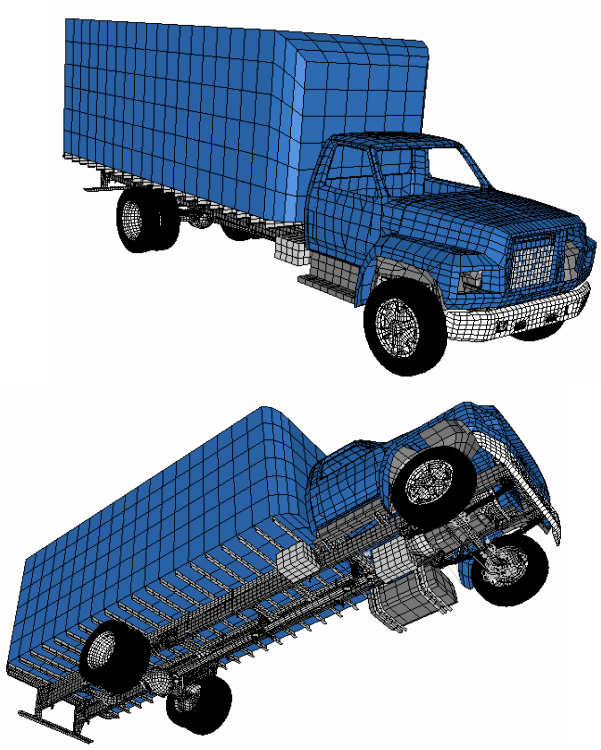

Figure 26: Ford 80 Truck Finite Element Model

The medium weight Ford Truck model in Figure 26 has been imported into the FEM models of the four example bridges separately in LS-DYNA. The whole bridge-vehicle model for collision simulations is shown in Figure 27. Since the ground level is 3 feet above the top surface of the bridge footing, the truck model has been moved up by 3 feet, as shown in Figure 28, so that the wheel bottom could contact the ground and move on the ground level.

It is reported that the impact angle of the truck hitting the bridge across the highway ranges from 0^o to 45^o. However, impact angles of 0^o and 45^o rarely occur [Cota (2007)]. In this research, the average value of 20^o has been chosen as the impact direction as shown in Figure 29. The truck model was rotated 20^o about the direction of the highway mid-line such that the mid-point of the truck head could first contact the bridge pier during the collision.

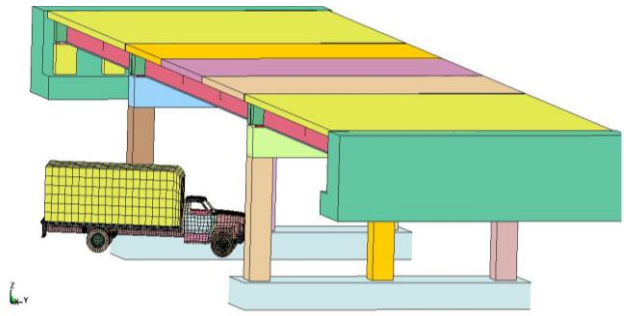

Figure 27: Numerical Model Representing the Impact Simulation between Ford Truck and Three-span Bridge

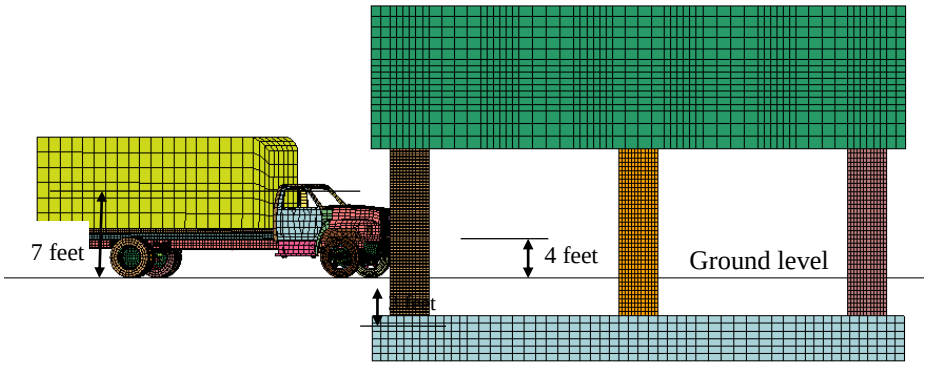

Figure 28: Elevation of the Ground Level with Truck Moving.

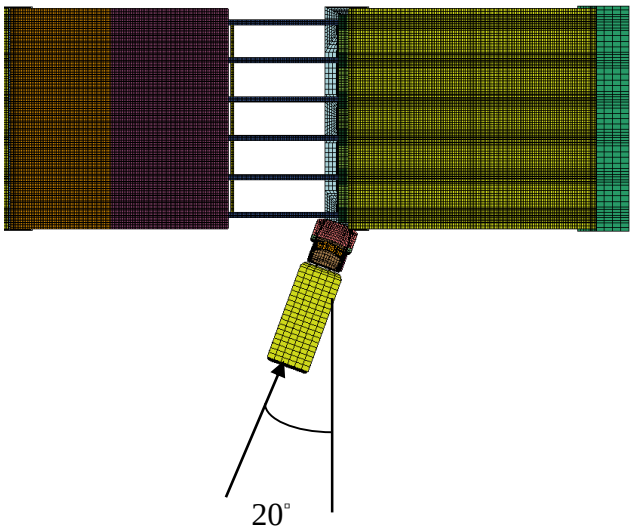

Figure 29: Impact Angle of Vehicle-bridge Collision

The range of the truck velocity in the collision is between the 40 and 65 miles/hour based on statistics assembled from collision accidents [Cota (2007)]. In order to carry out a parametric study on various impact velocities, impact velocities of the truck are set as 70 miles/hour, 50 miles/hour and 30 miles/hour.

6.1 Failure Modes of Bridge under Vehicular Impact

Results of three numerical simulations of vehicle-bridge collision have been analyzed to (i) identify various failure mechanisms, and (ii) capture time histories of the deformation and impact contact forces during collisions.

The simulation result shows that the NY Bridge piers undergo severe damages when impacted by the truck at 70 MPH velocity.

- Both cover and core concrete in the pier have cracked; concrete and reinforcement debond.
- Both footing and bent experience sudden pull forces towards the impact area on the pier because of a sudden large lateral impact force acting on the longitudinal rebars. The impact force is transmitted to the bent as a sudden downward pull force before longitudinal rebars are ruptured.
- Under the combined gravity load of the superstructure and the pull force caused by impact, the bent acts as a lever beam. Consequently, a plastic hinge is observed to form at the joint of the interior column with the bent as shown in Figure 30.

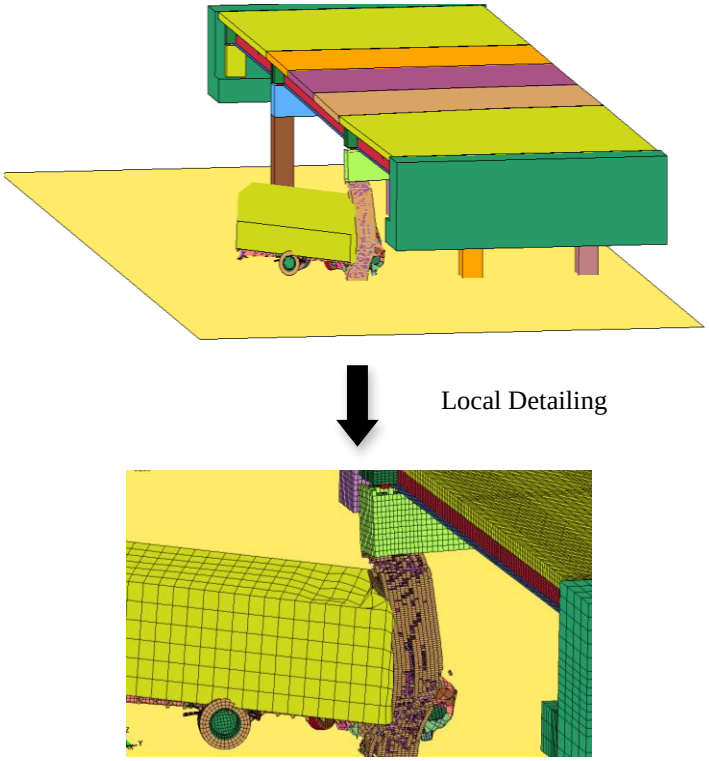

Figure 30: Failure Mechanism of the Whole Bridge-Vehicle Collision (NY-70).

The exterior pier in the NY bridge under 70 MPH impact velocity loses its capacity after the rupture of longitudinal rebars. Based on the simulation results, six types of failure mechanisms, labeled as A1 to A6, shown in Figures 31 to 40, have been identified.

Damage Mechanism A1. Spalling of Concrete Surface: During the impact load on concrete surface of a pier, some of the stress waves are reflected back from the pier surface. This causes a tensile wave effect on the back surface of the pier, resulting in spalling of concrete as shown in Figure 31. Hence, spalling of concrete is usually more severe on the back surface of a pier than on the surface impacted by the vehicle. An example of spalling of concrete after an accidental impact on a bridge pier in Texas is shown in Figure 32.

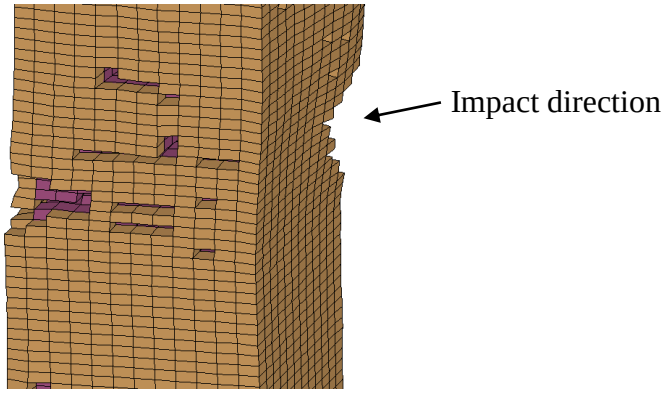

Figure 31: Damage Mechanism A1: Spalling of Concrete Surface and Damage of Pier Concrete Core

Figure 32: Spalling of Concrete Pier in the Collision Accident of Tyler, Texas (2004).

Damage Mechanism A2. Breakage of Pier: Breakage of piers, as illustrated in Figure 33, can occur either because of flexural failure, or shear failure. In case of truck impacts on bridge piers, shear failure is more prominent than flexural failure. This mechanism generally leads to a complete collapse of a bridge. An example of breakage of bridge pier after an accidental impact on a bridge pier is shown in Figure 34.

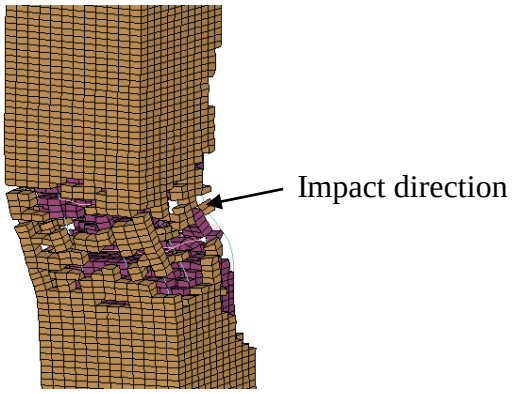

Figure 33: Damage Mechanism A2: Breakage of Pier

Figure 34: Breakage of Bridge Pier in the Collision Accident of Sealy, Texas (2004)

Damage Mechanism A3. Rebar Severance: If pier is tied well to the bent and the footing, the pier will tend to pull out from the footing and the bent because of stresses induced by the section change between the bent and the pier. This can cause severance of longitudinal rebars, as shown in Figure 35. Stirrups fail with the contact of the truck head as the concrete got eroded, as shown in Figure 36 for an accidental impact on piers in Texas.

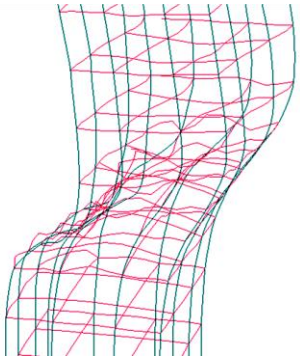

Figure 35: Damage Mechanism A3: Severance of Rebars in the Pier Steel Cage

Figure 36: Severance of Rebars in the Pier Steel Cage in the Collision Accident of Tyler, Texas (2004)

Damage Mechanism A4: Plastic Hinge Formation in the Pier: concrete core of piers is crushed under the impact of vehicular impact load, resulting in the formation of the plastic hinge in the piers at the location of impact contact and the joint between the bent and the column as shown in Figure 37. An example of plastic hinge formation in a pier hit by a truck in Minnesota is shown in Figure 38.

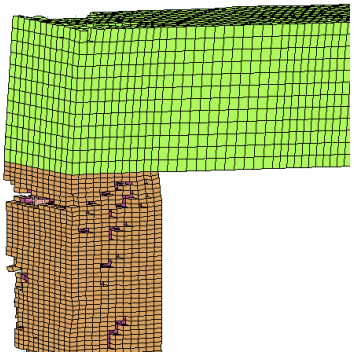

Figure 37: Damage Mechanism A4: Plastic Hinge Formation in the Pier

Figure 38: Plastic Hinge Formation in the Pier of 2003 Minnesota Collision Accident

Damage Mechanism A5. Concrete Crushing in the Bent: Concrete near the connection between bent and pier may be crushed because of stress concentration as shown in Figure 39.

Damage Mechanism A6. Flexural Failure of the Bent: After a bridge pier loses its load carrying capacity because of plastic hinge formation, most of the weight of the superstructure is transferred to the bent. Impact force is also transmitted to the bent as a downward pull force by longitudinal rebars extending into the bent. Because of combined effects of these two loads, the bent acts like a lever beam with large sudden load, resulting in flexural failure at the connection between the bent and the interior pier, as shown in Figure 39. An example of damage to a bent of a bridge after a vehicular impact is shown in Figure 40.

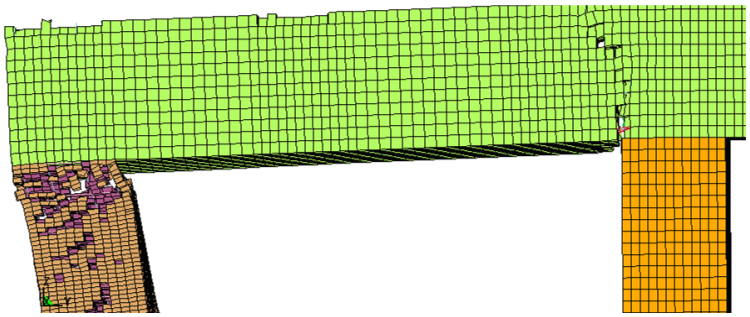

Figure 39: Damage Mechanism A5 and A6: Crush in the Bent and Flexural Failure of the Bent Beam

Figure 40: Damage of the Bent in the Collision Accident of Red Oak, Texas (2005)

6.2 Displacement Profiles and Impact Forces during Vehicular Impact

In order to evaluate the safety of highway bridge piers under vehicular impact loads, it is important to record and compare structural displacements and impact forces during bridge-vehicle impact simulations. It has been noted from observed failure mechanisms of bridges that the maximum deformation in a pier subject to truck impact occurs at mid-height of the pier. Hence, it is reasonable to capture the displacement of this location to characterize the behavior of a pier subject to vehicular impact. Figures 41 shows mid-height displacement time histories of the impacted pier. These displacement time histories can be used to study the influence of the impact velocity on bridge pier deformation. For the NY bridge pier subjected to impact by a truck with 70 mph velocity, it is observed from Fig 41 that the mid-height displacement of the pier starts to increase suddenly at time instant 0.11 seconds and reaches

the maximum value of 500mm at 0.25 seconds. In case of 50 mph impact velocity, mid-height displacement starts increasing at 0.16 seconds (time of impact) and reaches the maximum of 200 mm at 0.20 seconds. The value of mid-height displacement of the pier in the case of 30 mph impact velocity is quite low when compared with those for medium and high impact velocities. It is observed that the maximum displacement decreases more than 50% when the impact velocity is decreased from 70 mph to 50 mph.

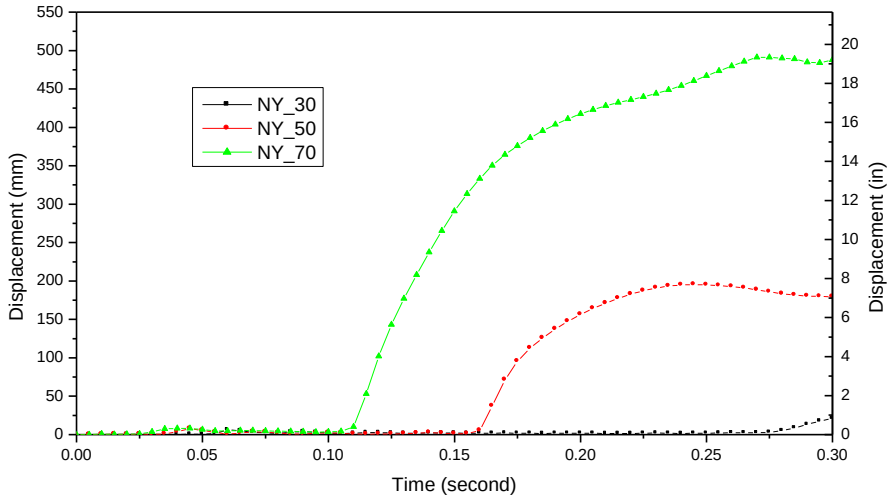

Figure 41: Mid-Pier Displacement Time Histories for the NY Bridge under Various Impact Velocities

7. Conclusion

In addition to natural hazards such as earthquake, flood and scour, highway bridge structures are also expected to withstand the human induced extreme events (such as blast, fires, vehicular impacts etc.) during their life time. After September 11, 2011 incident, safety of infrastructure systems has received heightened public concerns. Transportation infrastructures are considered to be attractive targets because of their accessibility and their potential impact to local economy and environment. A bridge engineer should prepare for the new generation of bridges and tunnels that are redundant and resilient to withstand unforeseen extreme events [Duwadi and Lwin (2006)]. This research focuses on the behavior and safety of highway bridge structures subject to vehicular impacts, which is considered to be the third leading cause of bridge failures in this country. This objective had been achieved by the numerical simulation of vehicular impact on a high fidelity finite element model of a highway bridge in LS-DYNA.

A typical three span simply supported bridge in New York State has been selected as an example bridge to investigate the behavior of highway bridge piers under vehicular impacts. Three dimensional high fidelity finite element model of the bridge has been developed based on the construction drawings. The concrete components are modeled with solid brick elements and rebars are modeled by beam elements. Both brick and beam elements are combined together through coinciding nodes shared by the two types of finite elements. The characteristic

mesh size of reinforced concrete in the impact area is set as 1 in based on verification of experimental results on impact testing of a beam in LS-DYNA.

Bridge models in LS-DYNA have been combined with a medium weight single unit truck model with approach velocities of 70 MPH, 50 MPH and 30 MPH. Simulation of 70 MPH impact velocity on the typical NY bridge has been carried out to identify all possible failure mechanisms, since this bridge is damaged severely when impacted by the truck moving at 70 MPH. Failure mechanisms captured are: spalling of concrete surface; breakage of the pier; severance of the longitudinal rebar and stirrups; plastic hinge formation in the pier; crush of the bent; and flexural failure of the bent. First two failure mechanism can be classified as repairable (minor) damage. Other failure mechanisms are classified as moderate to severe damage. After a vehicular impact, a bridge pier with minor damage can be repaired without replacement of the concrete component. A bridge pier with moderate damage may have to be repaired with structural rehabilitation. A severely damaged bridge pier may pose high risk of collapse of the bridge. Hence, the bridge may have to be demolished and reconstructed.

8. References

American Association of State Highway and Transportation Officials Load and Resistance Factor Design.(1998). *AASHTO-LRFD Bridge Design Specifications -fourth edition, AASHTO*, Washington, D.C.

American Association of State Highway and Transportation Officials Load and Resistance Factor Design.(2007). *AASHTO-LRFD Bridge Design Specifications -fourth edition , AASHTO*, Washington, D.C.

American Association of State Highway and Transportation Officials Load and Resistance Factor Design.(2007). *AASHTO Guide Specification for LRFD Seismic Bridge Design, AASHTO*, Washington, D.C.

Akram Abu-Odeh, Brackin M. S. (2008). *Guidelines for Designing Bridge Piers and Abutments for Vehicle Collisions-Phase I-Simulation Analysis*. College Station, Texas.

Anil K. Agrawal.(2008). *Multi-hazard Seismic-blast-impact Load Effects on Highway Bridges for Performance Based Design*. NJDOT Technology Transfer Seminar, Ewing, NJ.

Anil K. Agrawal.(2010). *Bridge Vehicle Impact Assessment.* University Transportation Research Center and New York State Department of Transportation(UTRC/NYSDOT).

Agrawal, A.K., Ghosn, M. And Alampalli, S. And Pan, Y. "Seismic Fragility of Retrofitted Multi-Span Continuous Steel Bridges in New York ", Accepted for publication in ASCE *Journal of Bridge Engineering*, 2011.

APTEK, Inc. (2007). *Evaluation of LS-DYNA Concrete Material Model 159*. Spring, Colorado .

Blejwas, T. E., Feng, C. C., Ayre, R. S.(1979). " Dynamic interaction of moving vehicles and structures*," Journal of Sound and Vibration,* Vol(67), 513-521.

Consolazio, G. (2005). "Barge Impact Testing at the St. George Island Bridge: Test Results & Design Implications". 2006 FICE/FDOT Design Conference, Orlando, Florida.

Consolazio, G. R. and Cowan, D. R. (2003). "Nonlinear analysis of barge crush behavior and its relationship to impact resistant bridge design," *Computers and Structures*, V(81):547-557.

Fujikura, S., Bruneau, M., Lopez-Garcia, D.(2008). "Experimental Investigation of Multihazard Resistant Bridge Piers Having Concrete-Filled Steel Tube under Blast Loading," *Journal of Bridge Engineering*, Vol(13), No.6.

Fujikake K., Li B. (2009). "Impact Response of Reinforced Concrete Beam and Its Analytical Evaluation". *Journal of Structural Engineering*, Vol.135(2009), No. 8.

Hargrave, M. W., Munley, E. and Pasko, T. J. (1997). "Federal Highway Administration's (FHWA's) applied highway infrastructure research program on composite materials," *Public Road Magzine*(TFHRC),Spring 1997, Vol(60): No. 4.

Holmquist, T., J., Johnson, G. R. and Cook W. H. (1993). "A Computational constitutive model for concrete subjected to large strains, high strains rates and high pressure." Presented at Fourth International Symposium on Ballistics. Quebec City, Canada, September 1993.

Kwasniewskia, L., Li Hongyi and Wekezerb, J. (2006). "Finite element analysis of vehicle-bridge interaction," *Finite Elements in Analysis and Design*, Vol(42): 950-959.

Krauthammer, T. & Otani, R. K.(1997). "Mesh, gravity and load effects on finite element simulations of blast loads reinforced concrete structures", *Computers and Structures*, V63(6), 1113.

Kishi N., Nakano O. (2001)."Experimental Study on Ultimate Strength of Flextural-Railure-Type RC Beams under Impact Loading", *Transactions, SMiRT16*, Washington DC.

LS-DYNA. (2007). *Theory manual for version 971* (2007). Livermore Software Technology Corporation, Livermore.

LS-DYNA.(2007). *LS-DYNA key word user's manual*, Livermore Software Technology Corporation, Livermore.

Miele, C.R., Plaxico, C. A., and Kennedy, J.C.(2005). *Heavy Vehicle-infrastructure asset interaction and Collision*. Heavy Vehicle Research Center, Oak Ridge National Laboratory.

Murray, Y. D.(2004). "Theory and Evaluation of Concrete Material Model 159". 8th International LS-DYNA Users Conference for Material Technology. Dearborn, MI.

Murray, Y. D. (2007). *User manual for LS-DYNA Concrete Material Model 159*. Federal Highway administration Turner-Fair bankhighway research center, Mclean, VA.

New York Sate Department of Transportation. (1996). *Bridge safety assurance, Collision Vulnerability Manual*, Albany, New York.

National Transportation Research Center & Heave Vehicle Research Center. (2005). *Heavy Vehicle Infrastructure Asset Interaction and Collision*. University of Tennessee Knoxville

Nam, J. W., Kim, J. J. and Kim S. B. (2008). "A study on Mesh Size Dependency of Finite Element Blast Structural Analysis Induced by Non-uniform Pressure Distribution from High Explosive Wave," *KSCE Journal of Civil Engineering*, (2008) 12(4):259-265.

Priestley M. and Seible F. (1996), *Seismic Design and Retrofit of Bridges*, John Wiley &Sons, Inc.

Sherif EI-Tawil and Edward S. (2005). "Vehicle Collision with Bridge Piers," *Journal of Structure Engineering*, Vol(10), pp 345-353.

Texas Transportation Institute. (2008). *Guidelines for Designing Bridge Piers and Abutments for Vehicle Collisions*, College Station, Texas.

Wardhana, K. and Hadipriono F.C.(2003). "Analysis of Recent Bridge Failures in the United States," *Journal of Performance of Constructed Facilities*, Vol.17, No.3.

Woisin G.(1976). "The collision tests of the GKSS," *Jahrbuch Schiffbautech Gesellsch*, 1976,V70:465-487.

Xiao Y., Liu C.L.(2010), "Study of Anti-Ram Bollards Based on Truck Collision Testing. ", *Proceeding of International Symposium on life-Cycle Performance of Bridges and Structures*, Science Press, Hunan.

Yang,Y.B., Liao, S.S., Lin, B.H. (1995). "Impact formulas for vehicles moving over simple and continuous beams," *Journal of Structural Engineering*, 121 (11):1644-1650.

Yang,Y.B. , Lin, B.H. (1995). "Vehicle–bridge interaction analysis by dynamic condensation method," *Journal of Structural Engineering*, 121 (11)1636–1643.

Yvonne D. M.& Roger Bligh,(2007). *Evaluation of LS-DYNA Concrete Material Model 159*. Texas Transportation Institute, College Station, TX.

Zaouk, A. K. & Marzoughi, D.(1996). "Validation of a non-linear finite element vehicle model using multiple impact data," *Crashworthiness and occupant protection in transportation systems*, AMD,Vol(218): PP: 91–106. ASME, New York.

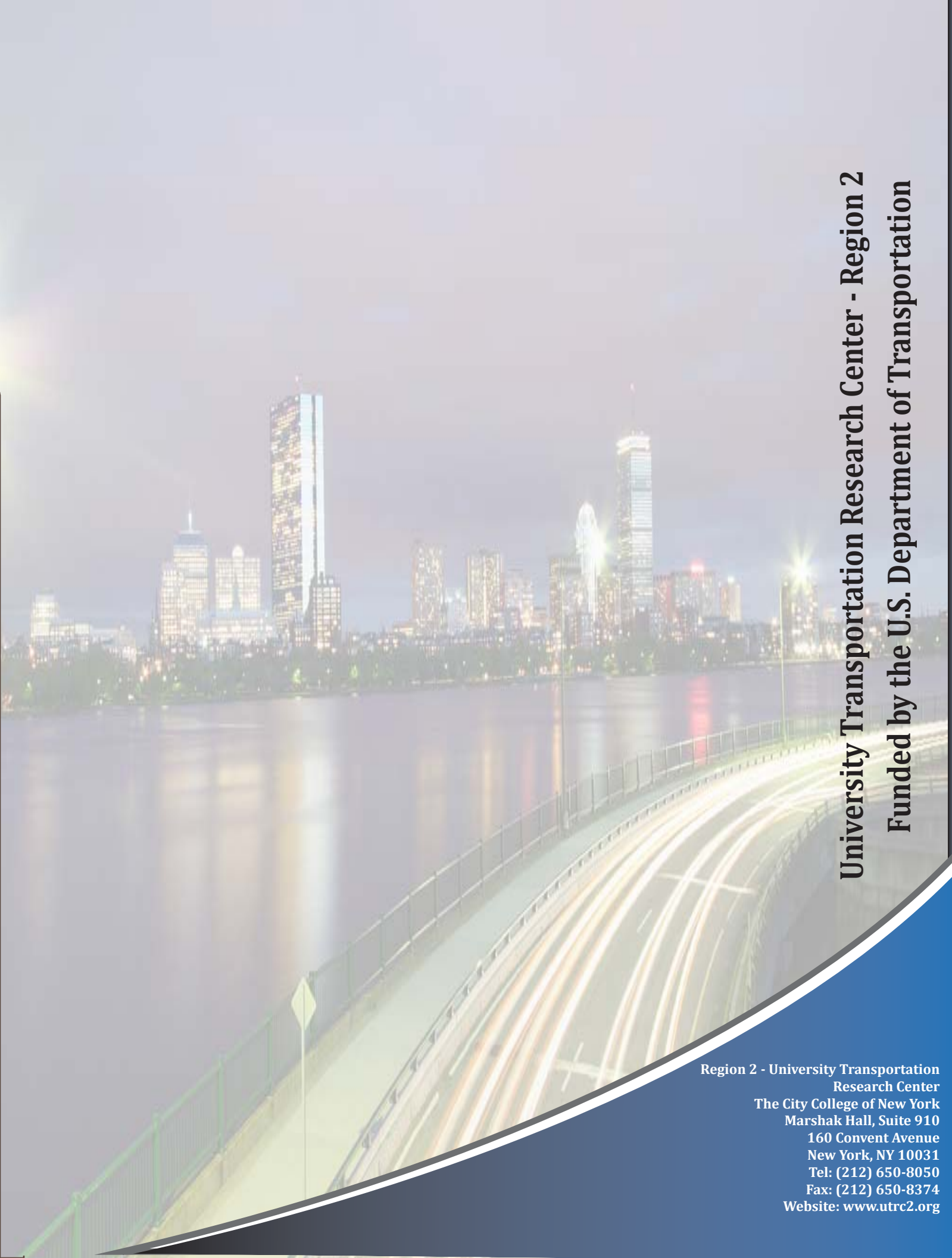

University Transportation Research Center - Region 2

Funded by the U.S. Department of Transportation

Region 2 - University Transportation
Research Center
The City College of New York
Marshak Hall, Suite 910
160 Convent Avenue
New York, NY 10031
Tel: (212) 650-8050
Fax: (212) 650-8374
Website: www.utrc2.org